LBL-38099
UC-414
Preprint

Lawrence Berkeley Laboratory
UNIVERSITY OF CALIFORNIA

Physics Division

Submitted to Physical Review D

The Muon Anomalous Magnetic Dipole Moment in the Minimal Supersymmetric Standard Model

T. Moroi

December 1995

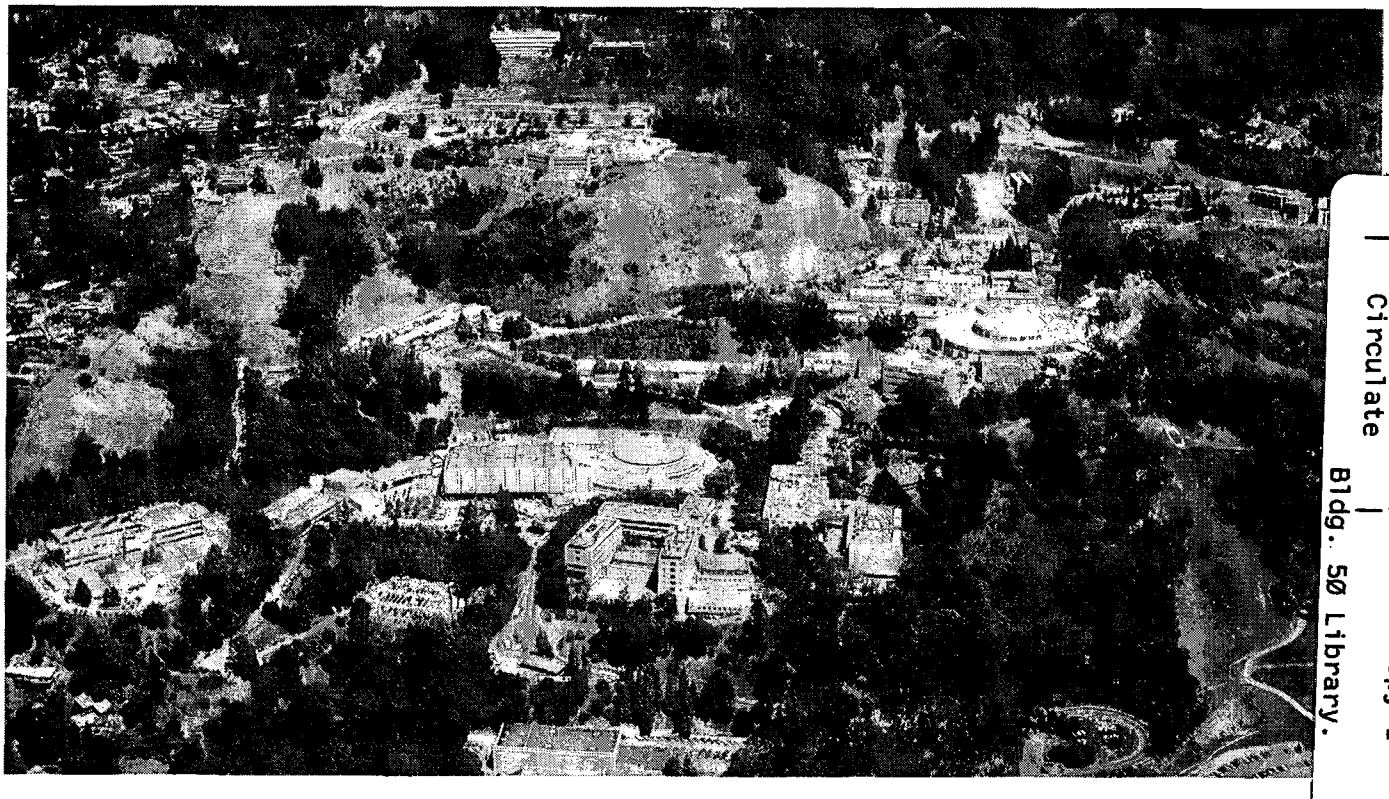

REFERENCE COPY
Does Not
Circulate
Bldg. 50 Library.
LBL-38099
Copy 1

Prepared for the U.S. Department of Energy under Contract Number DE-AC03-76SF00098

DISCLAIMER

This document was prepared as an account of work sponsored by the United States Government. While this document is believed to contain correct information, neither the United States Government nor any agency thereof, nor the Regents of the University of California, nor any of their employees, makes any warranty, express or implied, or assumes any legal responsibility for the accuracy, completeness, or usefulness of any information, apparatus, product, or process disclosed, or represents that its use would not infringe privately owned rights. Reference herein to any specific commercial product, process, or service by its trade name, trademark, manufacturer, or otherwise, does not necessarily constitute or imply its endorsement, recommendation, or favoring by the United States Government or any agency thereof, or the Regents of the University of California. The views and opinions of authors expressed herein do not necessarily state or reflect those of the United States Government or any agency thereof or the Regents of the University of California.

LBL-38099
hep-ph/9512396
Dec. 1995

The Muon Anomalous Magnetic Dipole Moment in the Minimal Supersymmetric Standard Model †

Takeo Moroi‡

Theoretical Physics Group, Lawrence Berkeley National Laboratory
University of California, Berkeley, CA 94720, U.S.A.

Abstract

The muon anomalous magnetic dipole moment (MDM) is calculated in the framework of the minimal supersymmetric standard model (MSSM). In this paper, we discuss how the muon MDM depends on the parameters in MSSM in detail. We show that the contribution of the superparticle-loop becomes significant especially when $\tan\beta$ is large. Numerically, it becomes $O(10^{-8} - 10^{-9})$ in a wide parameter space, which is within the reach of the new Brookhaven E821 experiment.

†This work was supported by the Director, Office of Energy Research, Office of High Energy and Nuclear Physics, Division of High Energy Physics of the U.S. Department of Energy under Contract DE-AC03-76SF00098.

‡E-mail address : moroi@theor3.lbl.gov

1 Introduction

Supersymmetry (SUSY) [1] is one of the most attractive candidates of the new physics beyond the standard model. In SUSY models, quadratic divergences are automatically canceled out, and hence SUSY may be regarded as a solution to the naturalness problem [2]. In addition, precision measurements of the gauge coupling constants strongly suggest SUSY grand unified theory (GUT) [3]. Contrary to our theoretical interests, however, evidences of SUSY (especially, superpartners) have not discovered yet, and hence superpartners are fascinating targets of the forthcoming high energy experiments like LEP II, LHC and NLC.

Even if we do not have high energy colliders, we can constrain SUSY models by using precision measurements in low energy experiments. This is because superparticles contribute to low energy physics through radiative corrections. Especially, superparticles are assumed to have masses of the order of the electroweak scale, and hence their loop effects may become comparable to those of $W^{\pm}$- or Z-boson propagations. Therefore, low energy precision experiments are also very useful to obtain constraints on SUSY models.

One of the quantities which are measured in a great accuracy is the muon anomalous magnetic dipole moment (MDM), $a_\mu \equiv \frac{1}{2}(g-2)_\mu$. At present, the muon MDM is measured to be [4]

$$a_\mu^{\rm exp} = 1165923(8.4) \times 10^{-9}. \tag{1}$$

On the other hand, the standard model prediction on a_μ is given by [5]

$$a_\mu^{\rm SM} = 116591802(153) \times 10^{-11}, \tag{2}$$

which is completely consistent with experimental value. (For a review of the calculation of $a_\mu^{\rm SM}$, see also Ref. [6].)

Because of the great accuracy of $a_\mu^{\rm exp}$ and $a_\mu^{\rm SM}$ given above, we can derive a constraint on SUSY models from the muon MDM. Furthermore, the new Brookhaven E821 experiment [7] is supposed to reduce the error of the experimental value of a_μ to 0.4×10^{-9}, which is smaller than the present one by a factor ~ 20. The accuracy of the Brookhaven E821 experiment is of the order of the contribution of the $W^{\pm}$- and Z-boson loop, which

means we may have a chance to measure the SUSY contribution to the muon MDM by that experiment.

In fact, there are several works in which the muon MDM is calculated in the framework of SUSY models [8, 9, 10]. Especially, Chattopadhyay and Nath recently pointed out that the muon MDM is a powerful probe of the models based on supergravity if $\tan\beta$ is large [10]. However, most of the recent works assume the boundary conditions on the SUSY breaking parameters based on the minimal supergravity, and/or radiative electroweak symmetry breaking condition, and hence it is quite unclear for us how the SUSY contributions to the muon MDM depends on the parameters in MSSM. Thus, the aim of this paper is to clarify it, and to investigate the behavior of the muon MDM in the framework of MSSM. The mass matrices and mixing angles among the superparticles have model dependence even if we assume the boundary condition based on the minimal supergravity, and hence we believe that it is important to analyze the muon MDM in a more general framework of the SUSY standard model.

In this paper, we investigate the SUSY contribution to the muon MDM in the framework of MSSM as a low energy effective theory of SUSY GUT [11]. The organization of this paper is as follows. In the next section, we introduce a model we consider. In Section 3, we show analytic forms of the SUSY contribution to the muon MDM, $\Delta a_\mu^{\rm SUSY}$. In Section 4, typical behavior of $\Delta a_\mu^{\rm SUSY}$ is discussed. In Section 5, some numerical results are shown. Section 6 is devoted to discussion.

2 Model

First of all, we would like to introduce a model we consider, *i.e.* MSSM as a low energy effective theory of SUSY GUT. All the field we use in our analysis is

$$l_L = (\mu_L\ \nu), \quad \mu_R^c, \quad H_1 = (H_1^-\ H_1^0), \quad H_2 = \begin{pmatrix} H_2^+ \\ H_2^0 \end{pmatrix}, \tag{3}$$

where l_L $(\mathbf{2}^*, -\frac{1}{2})$ and μ_R^c $(\mathbf{1}, 1)$ are left- and right-handed muon, while two Higgs doublets are represented as H_1 $(\mathbf{2}^*, -\frac{1}{2})$ and H_2 $(\mathbf{2}, \frac{1}{2})$. (We denote the quantum numbers for the $\mathrm{SU(2)_L} \times \mathrm{U(1)_Y}$ gauge group in the parenthesis.) The Higgs doublets H_1 and H_2 are responsible for the electroweak symmetry breaking, and hence their vacuum-expectation

values are constrained as $\langle H_1\rangle^2 + \langle H_2\rangle^2 \simeq (174\text{GeV})^2$ in order to give a correct value of the Fermi constant. On the other hand, the ratio of the vacuum-expectation values of two Higgs doublets is a free parameter in MSSM, which we define $\tan\beta \equiv \langle H_2\rangle/\langle H_1\rangle$.

Relevant part of the superpotential of MSSM is given by

$$W = y_\mu \epsilon^{\alpha\beta} \mu_R^c l_{L,\alpha} H_{1,\beta} + \mu_H H_{1,\alpha} H_2^\alpha, \tag{4}$$

where y_μ is the Yukawa coupling constant of muon, μ_H the SUSY invariant Higgs mass and $\epsilon^{\alpha\beta}$ the anti-symmetric tensor with $\epsilon^{12} = 1$. Using the superpotential given above, F-term contribution to the lagrangian is obtained as

$$\mathcal{L}_F = -\int d^2\theta W + h.c. \tag{5}$$

Furthermore, soft SUSY breaking terms are given by

$$\begin{aligned}\mathcal{L}_{\text{soft}} &= -m_L^2 \tilde{l}_L^* \tilde{l}_L - m_R^2 \tilde{\mu}_R^{c*} \tilde{\mu}_R^c - (A_\mu \epsilon^{\alpha\beta} \tilde{\mu}_R^c \tilde{l}_{L,\alpha} H_{2,\beta} + h.c.) \\ &\quad -\frac{1}{2}(m_{G2} \tilde{W}\tilde{W} + m_{G1} \tilde{B}\tilde{B} + h.c.).\end{aligned} \tag{6}$$

Here, $\tilde{l}_L$, $\tilde{\mu}_R$, $\tilde{W}$ and $\tilde{B}$ represent left- and right-handed sleptons in second generation, and gauginos for SU(2)_L and U(1)_Y gauge group, respectively. Gaugino masses m_{G1} and m_{G2} are related by the GUT relation;

$$\frac{m_{G2}}{g_2^2} = \frac{3}{5}\frac{m_{G1}}{g_1^2}, \tag{7}$$

where g_1 and g_2 are the gauge coupling constant of SU(2)_L and U(1)_Y gauge group, respectively.[1]

Here, we should comment on a flavor mixing in slepton mass matrices. If there is a large flavor mixing in the slepton mass matrices, all the sleptons contribute to the muon MDM. However, flavor mixing in the slepton mass matrices may be dangerous, since it induces a lepton flavor violation processes such as $\mu \to e\gamma$, $\tau \to \mu\gamma$ and so on. Especially, the mixing among first and second generation is severely constrained from $\mu \to e\gamma$ especially when $\tan\beta$ is large [13]. On the other hand, the constraint on the mixing of the second and third generation is not so stringent. In this paper, for simplicity, we assume that the

[1]The GUT relation given in eq.(7) holds in general if the gauge groups are unified in a larger group [12]. Therefore, we are not depending on specific model of GUT.

flavor mixing in the slepton mass matrix is not so large, and that it does not affect the following arguments. A comment on the case with the flavor mixing is given in Section 6.

Once we have the MSSM lagrangian, we can obtain mass eigenvalues and mixing matrices of the superparticles. The mass matrix for the smuon field is given by

$$M^2_{\tilde{\mu}} = \begin{pmatrix} m^2_{\tilde{\mu}L} & m^2_{LR} \\ m^2_{LR} & m^2_{\tilde{\mu}R} \end{pmatrix}, \tag{8}$$

where

$$\begin{aligned} m^2_{\tilde{\mu}L} &= m^2_L + m^2_Z \cos 2\beta \left(\sin^2\theta_W - \frac{1}{2}\right), && (9) \\ m^2_{\tilde{\mu}R} &= m^2_R - m^2_Z \cos 2\beta \sin^2\theta_W, && (10) \\ m^2_{LR} &= y_\mu \mu_H \langle H_2 \rangle + A_\mu \langle H_1 \rangle. && (11) \end{aligned}$$

The mass matrix $M^2_{\tilde{\mu}}$ can be diagonalized by using an unitary matrix $U_{\tilde{\mu}}$ as

$$(U^\dagger_{\tilde{\mu}} M^2_{\tilde{\mu}} U_{\tilde{\mu}})_{AB} = m^2_{\tilde{\mu}A}\delta_{AB} \quad (A, B = 1, 2), \tag{12}$$

where $m_{\tilde{\mu}A}$ is the mass eigenvalue of the smuon. Notice that, in our case, off-diagonal element of the mass matrix given in eq.(8) is substantially smaller than the diagonal elements, and hence $m_{\tilde{\mu}L}$ and $m_{\tilde{\mu}R}$ almost correspond to the mass eigenvalues. The mass of the sneutrino, $m_{\tilde{\nu}}$, is also easily obtained as

$$m^2_{\tilde{\nu}} = m^2_L + \frac{1}{2} m^2_Z \cos 2\beta. \tag{13}$$

Next, we derive the mass matrices for neutralinos and charginos. For neutralinos, the mass terms are given by

$$\begin{aligned} \mathcal{L}_{\chi^0} &= -\frac{1}{2}(i\tilde{B}\ i\tilde{W}^3\ \tilde{H}^0_1\ \tilde{H}^0_2) \\ &\begin{pmatrix} -m_{G1} & 0 & -\frac{1}{\sqrt{2}}g_1\langle H_1\rangle & \frac{1}{\sqrt{2}}g_1\langle H_2\rangle \\ 0 & -m_{G2} & \frac{1}{\sqrt{2}}g_2\langle H_1\rangle & -\frac{1}{\sqrt{2}}g_2\langle H_2\rangle \\ -\frac{1}{\sqrt{2}}g_1\langle H_1\rangle & \frac{1}{\sqrt{2}}g_2\langle H_1\rangle & 0 & \mu_H \\ \frac{1}{\sqrt{2}}g_1\langle H_2\rangle & -\frac{1}{\sqrt{2}}g_2\langle H_2\rangle & \mu_H & 0 \end{pmatrix} \begin{pmatrix} i\tilde{B} \\ i\tilde{W}^3 \\ \tilde{H}^0_1 \\ \tilde{H}^0_2 \end{pmatrix} \\ &+ h.c., \end{aligned} \tag{14}$$

where $\tilde{H}_1$ and $\tilde{H}_2$ represent the higgsino field. Then, we can find an unitary matrix U_{χ^0} which diagonalize the mass matrix given above. Denoting the mass matrix given in eq.(14)

as M_{χ^0}, mass eigenvalues for the neutralino field, $m_{\chi^0 X}$, is given by

$$(U^\dagger_{\chi^0} M_{\chi^0} U_{\chi^0})_{XY} = m_{\chi^0 X}\delta_{XY} \quad (X, Y = 1-4). \tag{15}$$

Similarly, mass terms for the charginos are given by

$$\mathcal{L}_{\chi^\pm} = -(\tilde{W}^+ \ \tilde{H}_2^+)\begin{pmatrix} -m_{G2} & g_2\langle H_1\rangle \\ -g_2\langle H_2\rangle & \mu_H \end{pmatrix}\begin{pmatrix} \tilde{W}^- \\ \tilde{H}_1^- \end{pmatrix} + h.c. \ , \tag{16}$$

with $\tilde{W}^\pm \equiv -\frac{i}{\sqrt{2}}(\tilde{W}^1 \mp i\tilde{W}^2)$. The mass matrix given in eq.(16), which we denote $M_{\chi^\pm}$, can be diagonalized by using two unitary matrices, U_{χ^+} and U_{χ^-};

$$(U^\dagger_{\chi^+} M_{\chi^\pm} U_{\chi^-})_{XY} = m_{\chi^\pm X}\delta_{XY} \quad (X, Y = 1, 2), \tag{17}$$

where $m_{\chi^\pm X}$ represents the mass eigenvalue of the chargino field.

With the coupling constants and mixing matrices given above, we can write down muon-neutralino-smuon and muon-chargino-sneutrino vertices. Denoting the mass eigenstates of the smuon, neutralino and chargino as $\tilde{\mu}_A$, χ^0_X and $\chi^\pm_X$, respectively, the interaction terms are given by

$$\mathcal{L}_{\rm int} = \sum_{AX} \bar{\mu}(N^L_{AX}P_L + N^R_{AX}P_R)\chi^0_X\tilde{\mu}_A + \sum_X \bar{\mu}(C^L_X P_L + C^R_X P_R)\chi^\pm_X\tilde{\nu} + h.c. \ , \tag{18}$$

where $P_L = \frac{1}{2}(1-\gamma_5)$, $P_R = \frac{1}{2}(1+\gamma_5)$ and

$$N^L_{AX} = -y_\mu(U_{\chi^0})_{3X}(U_{\tilde{\mu}})_{LA} - \sqrt{2}g_1(U_{\chi^0})_{1X}(U_{\tilde{\mu}})_{RA}, \tag{19}$$

$$N^R_{AX} = -y_\mu(U_{\chi^0})_{3X}(U_{\tilde{\mu}})_{RA} - \frac{1}{\sqrt{2}}g_2(U_{\chi^0})_{2X}(U_{\tilde{\mu}})_{LA} - \frac{1}{\sqrt{2}}g_1(U_{\chi^0})_{1X}(U_{\tilde{\mu}})_{LA}, \tag{20}$$

$$C^L_X = y_\mu(U_{\chi^-})_{2X}, \tag{21}$$

$$C^R_X = -g_2(U_{\chi^+})_{1X}. \tag{22}$$

By using the interaction terms given in eq.(18), we calculate the SUSY contribution to the muon MDM.

3 Analytic formulae

Now, we are in position to calculate the SUSY contribution to the muon MDM. What we have to calculate is the "magnetic moment type" operator, which is given by

$$\mathcal{L}_{\rm MDM} = \frac{e}{2m_\mu}F_2\bar{\mu}\sigma_{\rho\lambda}\mu F^{\rho\lambda}, \tag{23}$$

where $\sigma_{\rho\lambda} = \frac{i}{2}[\gamma_\rho, \gamma_\lambda]$, $F_{\rho\lambda}$ is the field strength of the photon field and F_2 the magnetic form factor. Muon anomalous magnetic moment, a_μ, is related to F_2 as

$$a_\mu = F_2. \tag{24}$$

Thus, by calculating magnetic form factor in the framework of MSSM, we can have SUSY contribution to the muon MDM.

In SUSY model, there are essentially two types of diagrams which contribute to a_μ, *i.e.* one is the neutralino (χ^0)-smuon ($\tilde{\mu}$) loop diagram (Fig. 1a) and the other is the chargino ($\chi^\pm$)-sneutrino ($\tilde{\nu}$) loop diagram (Fig. 1b);

$$\Delta a_\mu^{\rm SUSY} = \Delta a_\mu^{\chi^0\tilde{\mu}} + \Delta a_\mu^{\chi^\pm\tilde{\nu}}. \tag{25}$$

Here, contribution from the χ^0-$\tilde{\mu}$ diagram, $\Delta a_\mu^{\chi^0\tilde{\mu}}$, is

$$\begin{aligned}
\Delta a_\mu^{\chi^0\tilde{\mu}} &= m_\mu \sum_{AX} \Big\{ - m_\mu (N_{AX}^L N_{AX}^L + N_{AX}^R N_{AX}^R) m_{\tilde{\mu}A}^2 J_5(m_{\chi^0 X}^2, m_{\tilde{\mu}A}^2, m_{\tilde{\mu}A}^2, m_{\tilde{\mu}A}^2, m_{\tilde{\mu}A}^2) \\
&\quad + m_{\chi^0 X} N_{AX}^L N_{AX}^R J_4(m_{\chi^0 X}^2, m_{\chi^0 X}^2, m_{\tilde{\mu}A}^2, m_{\tilde{\mu}A}^2) \Big\} \\
&= \frac{1}{16\pi^2} m_\mu \sum_{AX} \Bigg\{ - \frac{m_\mu}{6 m_{\tilde{\mu}A}^2 (1 - x_{AX})^4} (N_{AX}^L N_{AX}^L + N_{AX}^R N_{AX}^R) \\
&\quad \times (1 - 6x_{AX} + 3x_{AX}^2 + 2x_{AX}^3 - 6x_{AX}^2 \ln x_{AX}) \\
&\quad - \frac{m_{\chi^0 X}}{m_{\tilde{\mu}A}^2 (1 - x_{AX})^3} N_{AX}^L N_{AX}^R (1 - x_{AX}^2 + 2x_{AX} \ln x_{AX}) \Bigg\},
\end{aligned} \tag{26}$$

where we are using mass eigenstate basis of χ^0 and $\tilde{\mu}$ (and that of $\chi^\pm$ in deriving eq.(29)). Here, $x_{AX} = m_{\chi^0 X}^2 / m_{\tilde{\mu}A}^2$, and we define the functions I_N and J_N as

$$I_N(m_1^2, \cdots, m_N^2) = \int \frac{d^4k}{(2\pi)^4 i} \frac{1}{(k^2 - m_1^2) \cdots (k^2 - m_N^2)}, \tag{27}$$

$$J_N(m_1^2, \cdots, m_N^2) = \int \frac{d^4k}{(2\pi)^4 i} \frac{k^2}{(k^2 - m_1^2) \cdots (k^2 - m_N^2)}. \tag{28}$$

Some useful formulae concerning the functions I_N and J_N are shown in Appendix A. Contribution from the $\chi^\pm$-$\tilde{\nu}$ loop diagram is also easily calculated, and the result is given by

$$\Delta a_\mu^{\chi^\pm\tilde{\nu}} = m_\mu \sum_X \Big[2m_\mu (C_X^L C_X^L + C_X^R C_X^R) \{ J_4(m_{\chi^\pm X}^2, m_{\chi^\pm X}^2, m_{\chi^\pm X}^2, m_{\chi^\pm X}^2)$$

$$
\begin{aligned}
&+m_{\tilde{\nu}}^2 J_5(m_{\chi^\pm X}^2, m_{\chi^\pm X}^2, m_{\chi^\pm X}^2, m_{\chi^\pm X}^2, m_{\tilde{\nu}}^2) - J_4(m_{\chi^\pm X}^2, m_{\chi^\pm X}^2, m_{\chi^\pm X}^2, m_{\tilde{\nu}}^2)\} \\
&-2m_X C_X^L C_X^R J_4(m_{\chi^\pm X}^2, m_{\chi^\pm X}^2, m_{\chi^\pm X}^2, m_{\tilde{\nu}}^2)\Big] \\
= \; & \frac{1}{16\pi^2} m_\mu \sum_X \left\{ \frac{m_\mu}{3m_{\tilde{\nu}}^2(1-x_X)^4}(C_X^L C_X^L + C_X^R C_X^R) \right. \\
&\times \left(1 + \frac{3}{2}x_X - 3x_X^2 + \frac{1}{2}x_X^3 + 3x_X \ln x_X\right) \\
&\left. -\frac{3m_{\chi^\pm X}}{m_{\tilde{\nu}}^2(1-x_X)^3} C_X^L C_X^R \left(1 - \frac{4}{3}x_X + \frac{1}{3}x_X^2 + \frac{2}{3}\ln x_X\right) \right\}, \qquad (29)
\end{aligned}
$$

where $x_X = m_{\chi^\pm X}^2 / m_{\tilde{\nu}}^2$.

4 Behavior of the SUSY contribution to the muon MDM

Before evaluating the SUSY contribution to the muon MDM numerically, we would like to discuss the behavior of $\Delta a_\mu^{\rm SUSY}$, especially in large $\tan\beta$ case. As we will soon see, $|\Delta a_\mu^{\rm SUSY}|$ becomes large as $\tan\beta$ increases. Thus, the discussion about the large $\tan\beta$ case will be helpful for us to understand the behavior of $\Delta a_\mu^{\rm SUSY}$.

For this purpose, it is more convenient to use the mass insertion method to calculate the penguin diagrams rather than working in the mass eigenstate basis of the superparticles which is used in the previous section. In the case where $\tan\beta$ is large, five diagrams dominantly contribute to $\Delta a_\mu^{\rm SUSY}$, which are shown in Fig. 2. Their contributions are given by

$$
\begin{aligned}
\Delta a_\mu^{\rm N1} &= g_1^2 m_\mu^2 m_{G1} \mu_H \tan\beta \\
&\quad \times \Big\{ J_5(m_{G1}^2, m_{G1}^2, m_{\tilde{\mu}L}^2, m_{\tilde{\mu}R}^2, m_{\tilde{\mu}R}^2) + J_5(m_{G1}^2, m_{G1}^2, m_{\tilde{\mu}L}^2, m_{\tilde{\mu}L}^2, m_{\tilde{\mu}R}^2) \Big\}, \qquad (30) \\
\Delta a_\mu^{\rm N2} &= \frac{1}{2} g_1^2 m_\mu^2 m_{G1} \mu_H \tan\beta \\
&\quad \times \Big\{ J_5(m_{G1}^2, m_{G1}^2, \mu_H^2, m_{\tilde{\mu}L}^2, m_{\tilde{\mu}L}^2) + J_5(m_{G1}^2, \mu_H^2, \mu_H^2, m_{\tilde{\mu}L}^2, m_{\tilde{\mu}L}^2) \Big\}, \qquad (31) \\
\Delta a_\mu^{\rm N3} &= -g_1^2 m_\mu^2 m_{G1} \mu_H \tan\beta \\
&\quad \times \Big\{ J_5(m_{G1}^2, m_{G1}^2, \mu_H^2, m_{\tilde{\mu}R}^2, m_{\tilde{\mu}R}^2) + J_5(m_{G1}^2, \mu_H^2, \mu_H^2, m_{\tilde{\mu}R}^2, m_{\tilde{\mu}R}^2) \Big\}, \qquad (32) \\
\Delta a_\mu^{\rm N4} &= -\frac{1}{2} g_2^2 m_\mu^2 m_{G2} \mu_H \tan\beta \\
&\quad \times \Big\{ J_5(m_{G2}^2, m_{G2}^2, \mu_H^2, m_{\tilde{\mu}L}^2, m_{\tilde{\mu}L}^2) + J_5(m_{G2}^2, \mu_H^2, \mu_H^2, m_{\tilde{\mu}L}^2, m_{\tilde{\mu}L}^2) \Big\}, \qquad (33)
\end{aligned}
$$

$$\Delta a_\mu^{\rm C} = g_2^2 m_\mu^2 m_{G2}\mu_H \tan\beta \times\Big\{2I_4(m_{G2}^2, m_{G2}^2, \mu_H^2, m_{\tilde\nu}^2) - J_5(m_{G2}^2, m_{G2}^2, \mu_H^2, m_{\tilde\nu}^2, m_{\tilde\nu}^2) +2I_4(m_{G2}^2, \mu_H^2, \mu_H^2, m_{\tilde\nu}^2) - J_5(m_{G2}^2, \mu_H^2, \mu_H^2, m_{\tilde\nu}^2, m_{\tilde\nu}^2)\Big\}. \quad (34)$$

Here, eqs.(30) – (33) are χ^0-$\tilde\mu$ loop contributions, while eq.(34) represents the $\chi^\pm$-$\tilde\nu$ loop one. By using these expressions, the SUSY contribution to the muon MDM is approximately given by

$$\Delta a_\mu^{\chi^0\tilde\mu} \simeq \Delta a_\mu^{\rm N1} + \Delta a_\mu^{\rm N2} + \Delta a_\mu^{\rm N3} + \Delta a_\mu^{\rm N4}, \quad (35)$$

$$\Delta a_\mu^{\chi^\pm\tilde\nu} \simeq \Delta a_\mu^{\rm C}. \quad (36)$$

Notice that the SUSY contribution to the muon MDM given in eqs.(30) – (34) approximately correspond to the terms which are proportional to $N^L N^R$ or $C^L C^R$ (*i.e.* terms which have a chirality flip in internal fermion line) in the exact formulae given in eqs.(26) and (29).

The first thing we can learn from the above expressions is that all the terms given in eqs.(30) – (34) are proportional to $\tan\beta$ [9, 10]. This is due to the fact that the chirality is flipped not by hitting the mass of the external muon but by directly hitting the Yukawa coupling. This mechanism also occurs in the case of the lepton flavor violations [13]. Thus, $|\Delta a_\mu^{\rm SUSY}|$ becomes large as $\tan\beta$ increases, and we obtain severer constraint on the parameter space as $\tan\beta$ gets larger.

The second point we should mention is that the relation between the sign of $\Delta a_\mu^{\rm SUSY}$ and those of parameters in MSSM. The dominant SUSY contribution given in eqs.(30) – (34) are all proportional to $m_G\mu_H\tan\beta$ (with $m_G = m_{G1}, m_{G2}$ being gaugino mass). Thus, if we change the sign of this combination, $\Delta a_\mu^{\rm SUSY}$ also changes its sign. Furthermore, in the case where we assume GUT relation on the gaugino masses, we checked that $\Delta a_\mu^{\rm N1}$ or $\Delta a_\mu^{\rm C}$ dominates over other terms ($\Delta a_\mu^{\rm N2}$, $\Delta a_\mu^{\rm N3}$, $\Delta a_\mu^{\rm N4}$) in most of the parameter space. Here, both $\Delta a_\mu^{\rm N1}$ and $\Delta a_\mu^{\rm C}$ have the same sign as the combination $m_G\mu_H\tan\beta$. Therefore, $\Delta a_\mu^{\rm SUSY}$ becomes positive (negative) when the sign of the combination $m_G\mu_H\tan\beta$ is positive (negative).[2] In the next section, we will see that this relation really holds as a result of numerical calculations.

[2]If m_G or μ_H is small, this relation does not hold. This is mainly because that the mass insertion method breaks down in such a case. Furthermore, in such a case, we cannot ignore $\Delta a_\mu^{\rm N3}$ or terms which

Furthermore, we comment here that the contribution of $\chi^{\pm}$-$\tilde{\nu}$ loop diagram dominates over that of the χ^0-$\tilde{\mu}$ loop ones if all the masses of the superparticles are almost degenerate. For example, let us consider the extreme case where all the masses for the superparticles (m_{G1}, m_{G2}, μ_H, $m_{\tilde{\mu}L}$, $m_{\tilde{\mu}R}$, $m_{\tilde{\nu}}$) are the same. Denoting the masses of the superparticles $m_{\rm SUSY}$, contributions of the χ^0-$\tilde{\mu}$ and $\chi^{\pm}$-$\tilde{\nu}$ loop diagrams to the muon MDM is given by

$$\begin{aligned}
\Delta a_\mu^{\chi^0\tilde{\mu}} &\simeq \Delta a_\mu^{\rm N1} + \Delta a_\mu^{\rm N2} + \Delta a_\mu^{\rm N3} + \Delta a_\mu^{\rm N4} \\
&= \frac{1}{192\pi^2}\frac{m_\mu^2}{m_{\rm SUSY}^2}(g_1^2 - g_2^2)\tan\beta, \qquad (37)\\
\Delta a_\mu^{\chi^\pm\tilde{\nu}} &\simeq \Delta a_\mu^{\rm C} \\
&= \frac{1}{32\pi^2}\frac{m_\mu^2}{m_{\rm SUSY}^2} g_2^2 \tan\beta. \qquad (38)
\end{aligned}$$

From the above expressions, we can see that the $\chi^{\pm}$-$\tilde{\nu}$ loop contribution is substantially larger than that of χ^0-$\tilde{\mu}$ loop. Thus, $\chi^{\pm}$-$\tilde{\nu}$ loop gives dominant contribution, as in the case of minimal SUSY GUT based on the minimal supergravity [10]. However, we should note here that the $\chi^{\pm}$-$\tilde{\nu}$ loop dominance does not hold in general. In the next section, we will see the SUSY contribution to $\Delta a_\mu^{\rm SUSY}$ significantly depends on the right-handed smuon mass $m_{\tilde{\mu}R}$ in certain parameter regions.

5 Numerical Results

In this section, we numerically estimate $\Delta a_\mu^{\rm SUSY}$ by using eqs.(26) and (29). As we mentioned before, there are essentially six parameters on which $\Delta a_\mu^{\rm SUSY}$ depends, *i.e.* SU(2) gaugino mass m_{G2},[3] left- and right-handed smuon masses $m_{\tilde{\mu}L}$ and $m_{\tilde{\mu}R}$ (which essentially correspond to the soft SUSY breaking parameters m_L^2 and m_R^2, respectively), SUSY invariant Higgs mass μ_H, ratio of the vacuum-expectation values of the two Higgs doublets, $\tan\beta = \langle H_2\rangle/\langle H_1\rangle$, and SUSY breaking A-parameter for the smuon, A_μ. However, especially in the large $\tan\beta$ region where SUSY contribution to $\Delta a_\mu^{\rm SUSY}$ may become significantly large, $\Delta a_\mu^{\rm SUSY}$ is not sensitive to A_μ if $A_\mu \sim O(y_\mu \mu_H)$. This is because A_μ always appears in expressions in the combination of $(A_\mu + y_\mu\mu_H\tan\beta)$, as shown in eq.(11).

is not proportional to $\tan\beta$ (*i.e.* terms which are proportional to $N^L N^L$, $N^R N^R$, $C^L C^L$ and $C^R C^R$ in the exact formula given in eqs.(26) and (29)). In that case, the sign of $m_G \mu_H \tan\beta$ is not directly related to that of $\Delta a_\mu^{\rm SUSY}$.

[3]Gaugino mass for $U(1)_Y$ gauge group is determined by the GUT relation (7).

Therefore, in our analysis, we take $A_\mu = 0$.[4] Then, we take the other five parameters as free parameters and calculate the SUSY contribution to the muon MDM for a given set of parameters.

First, we show the SUSY contribution to the muon MDM for fixed values of $m_{\tilde{\mu}R}$ and $m_{\tilde{\mu}L}$ in μ_H-m_{G2} plane.[5] In Fig. 3, we plotted the results for $m_{\tilde{\mu}R} = 100$GeV and $\tan\beta = 30$. Here, the left-handed smuon mass is taken to be 100GeV (Fig. 3a), 300GeV (Fig. 3b) and 500GeV (Fig. 3c). The results for the cases of $m_{\tilde{\mu}R} = 300$GeV and $m_{\tilde{\mu}R} = 1$TeV are also shown in Fig. 4 and Fig. 5, respectively. As we can see, if we take a smaller value of $m_{\tilde{\mu}R}$, the SUSY contribution to the muon MDM is enhanced in the large μ_H region. This can be easily understood if we think of the fact that $\Delta a_\mu^{\rm N1}$ gives a large contribution in such a parameter region.

Furthermore, by choosing the right-handed smuon mass $m_{\tilde{\mu}R}$ so that $|\Delta a_\mu^{\rm SUSY}|$ is minimized, we obtain the lowerbound on the SUSY contribution to the muon MDM. The results are shown in Fig. 6. Here, we assume 45GeV $\leq m_{\tilde{\mu}R} \leq$ 1TeV. The lowerbound is obtained from the negative search for the smuon [4], while the upperbound is due to the naturalness point of view. In fact, the results are insensitive to the upperbound if we take the upperbound larger than about 1TeV, since the effects of the right-handed smuon decouple when we take $m_{\tilde{\mu}R} \to \infty$.

The SUSY contribution to the muon MDM has quite a complicated dependence on the parameters in MSSM. However, in a certain parameter space, $|\Delta a_\mu^{\rm SUSY}|$ becomes $O(10^{-8})$ which is of the order of the present accuracy of the measurement of the muon MDM.

Remember that the SUSY contribution to the muon MDM is approximately proportional to $\tan\beta$. Therefore, even for the case of $\tan\beta \neq 30$, we can read off the approximate value of $\Delta a_\mu^{\rm SUSY}$ from Fig. 3 – Fig. 6. For example, the contours for $\Delta a_\mu^{\rm SUSY} = 2 \times 10^{-9}$ in these figures correspond to $\Delta a_\mu^{\rm SUSY} \simeq 4 \times 10^{-9}$ for the case of $\tan\beta = 60$.

If the new Brookhaven E821 experiment measures the muon MDM with the accu-

[4]The supergravity model suggests $A_\mu \sim O(y_\mu m_{\tilde{\mu}})$ [14]. Furthermore, it was pointed out that some unwanted minimum appears in the potential of the smuon when $|A_\mu| > O(1) \times y_\mu m_{\tilde{\mu}}$ [15], which may cause cosmological difficulties. We checked that the results given in Fig. 3 – Fig. 7 are almost unchanged even if we take $A_\mu = 3 y_\mu m_{\tilde{\mu}L}$.

[5]Some regions of the μ_H-m_{G2} plane are excluded by the negative search for signals of neutralinos or charginos [16], though we do not show the excluded regions explicitly. Notice that, in our convention, the constraint becomes severer for the case of $\mu_H m_{G2} > 0$ rather than $\mu_H m_{G2} < 0$, as shown in Ref. [16].

racy of their proposal, it will give a great impact on MSSM. In a large parameter space, $|\Delta a_\mu^{\rm SUSY}|$ becomes $O(10^{-9})$, which is within the reach of the new Brookhaven E821 experiment. Furthermore, the theoretical uncertainty, which is almost originate to the hadronic uncertainty, is also expected to be decreased due to better measurements of the cross section of $e^+ + e^- \to$ hadrons at low energies. Thus, the muon MDM should be regarded as a good probe of MSSM.

Before comparing $\Delta a_\mu^{\rm SUSY}$ with constraint from experiment, we would like to discuss the behavior of $\Delta a_\mu^{\rm SUSY}$ shown in Fig. 6. As can be seen, $\Delta a_\mu^{\rm SUSY}$ changes its behavior at around $|\mu_H| \sim m_{\tilde{\mu}L}$. This can be understood in a following way. In the case of $|\mu_H| \sim m_{\tilde{\mu}L}$, $\Delta a_\mu^{\rm N1}$ and $\Delta a_\mu^{\rm N3}$ almost cancels out and $\Delta a_\mu^{\rm SUSY}$ becomes insensitive to $m_{\tilde{\mu}R}$. In the case of $|\mu_H| \gtrsim m_{\tilde{\mu}L}$, $m_{\tilde{\mu}R}$-dependence of $\Delta a_\mu^{\rm SUSY}$ is almost determined by that of $\Delta a_\mu^{\rm N1}$. Then, $|\Delta a_\mu^{\rm SUSY}|$ becomes smaller as $m_{\tilde{\mu}R}$ becomes larger. On the other hand, if $|\mu_H| \lesssim m_{\tilde{\mu}L}$, $\Delta a_\mu^{\rm N3}$ determines the $m_{\tilde{\mu}R}$-dependence of $\Delta a_\mu^{\rm SUSY}$. The important point is that the sign of $\Delta a_\mu^{\rm N3}$ is opposite to that of $\Delta a_\mu^{\rm C}$ which gives the dominant contribution. Thus, $|\Delta a_\mu^{\rm SUSY}|$ gets smaller as $m_{\tilde{\mu}R}$ decreases. In summary, in the case of $|\mu_H| \gtrsim m_{\tilde{\mu}L}$, $|\Delta a_\mu^{\rm SUSY}|$ increases as $m_{\tilde{\mu}R}$ decreases, while in the case of $|\mu_H| \lesssim m_{\tilde{\mu}L}$, $|\Delta a_\mu^{\rm SUSY}|$ decreases as $m_{\tilde{\mu}R}$ gets smaller.

The SUSY contribution should be compared with the accuracy of the present values of the experimental and theoretical values of the muon MDM, which are given in eqs.(1) and (2). Combining them, we obtain a constraint on the SUSY contribution to the muon MDM, $\Delta a_\mu^{\rm SUSY}$, which is given by

$$-9.0 \times 10^{-9} \leq \Delta a_\mu^{\rm SUSY} \leq 19.0 \times 10^{-9} \quad (90\% \text{ C.L.}). \tag{39}$$

In Fig. 7, we show the contour of $\tan\beta$ which gives the threshold value of the present constraint on $\Delta a_\mu^{\rm SUSY}$ given above (*i.e.* $\Delta a_\mu^{\rm SUSY} = -9.0 \times 10^{-9}$ and $\Delta a_\mu^{\rm SUSY} = 19.0 \times 10^{-9}$). Here, we choose $m_{\tilde{\mu}R}$ so that $|\Delta_\mu^{\rm SUSY} - 5.0 \times 10^{-9}|$ is minimized (where 5.0×10^{-9} is the center value of the constraint (39)). Thus, Fig. 7 should be regarded as a constraint on μ_H-m_{G2} plane for a fixed values of $m_{\tilde{\mu}L}$ and $\tan\beta$. Notice that if we assume a larger value of $\tan\beta$, SUSY contribution exceeds the present limit on the muon MDM in wider regions.

Before closing this section, we point out the fact that the contour in Fig. 7 is not

symmetric under $\mu_H \to -\mu_H$. This is because the center value of the constraint given in inequality (39) is 5.0×10^{-9}, which deviates from zero. Therefore, constraint (39) prefers positive value of $\Delta a_\mu^{\rm SUSY}$, and hence we have severer constraint for $\mu_H < 0$.

6 Discussion

In this paper, we investigated the SUSY contribution to the muon MDM by regarding all the parameters in MSSM as free parameters. Especially when $\tan\beta$ is large, the SUSY contribution is enhanced, and some parameter region of MSSM is excluded not to conflict with the present constraint on the muon MDM. In fact, even in the case where $\tan\beta$ is not so large ($\tan\beta \lesssim 10$), $\Delta a_\mu^{\rm SUSY}$ may become comparable to the present limit on the muon MDM, if the masses of the superparticles are quite light (see Fig. 6a).

Here, we would like to comment on the case with the flavor mixing in the slepton mass matrices. If the off-diagonal elements of the slepton mass matrices are substantially large, all the sleptons contribute to the muon MDM, as we mentioned before. However, for the case where the flavor mixing exists only in left- or right-handed lepton mass matrix, the previous arguments are almost unchanged. If both left- and right-handed slepton mass matrices have large off-diagonal elements, situation changes. Especially, in this case, Yukawa coupling constant of the tau can contribute to the muon MDM through the Feynman diagram like (N1) in Fig. 2, and hence the muon MDM may be enhanced.

Detailed analysis of this case is quite complicated since the muon MDM depends on a large number of parameters. Thus, we only discuss the case where the diagonal element of the left- and right-handed sleptons, $\hat{m}_L^2$ and $\hat{m}_R^2$, are proportional to unit matrix; $\hat{m}_{L,ii}^2 = m_L^2$, $\hat{m}_{R,ii}^2 = m_R^2$ (i: not summed). First, we consider the case where one of $\hat{m}_L^2$ or $\hat{m}_R^2$ has off-diagonal element. In this case, the results of the previous analysis are almost unaffected. For example, even if $\hat{m}_{L,23}^2/\hat{m}_{L,22}^2 = 0.5$ (or $\hat{m}_{R,23}^2/\hat{m}_{R,22}^2 = 0.5$), the correction to the $\Delta a_\mu^{\rm SUSY}$ is less than $\sim 10\%$. If both $\hat{m}_L^2$ and $\hat{m}_R^2$ have large off-diagonal elements, $\Delta a_\mu^{\rm SUSY}$ may receive a large correction. Numerically, when $\hat{m}_{L,23}^2/\hat{m}_{L,22}^2 \sim \hat{m}_{R,23}^2/\hat{m}_{R,22}^2 \sim 0.2$, the correction is $O(10\%)$. The correction gets larger as the off-diagonal elements increase.

The new Brookhaven E821 experiment will give a strong impact on SUSY models.

By the experiment, the muon MDM is expected to be measured with accuracy about 0.4×10^{-9}. Furthermore, the uncertainty in the theoretical prediction, which mainly comes from hadronic contributions, is hoped to be reduced by several experiments like VEPP-2M, DAΦNE and so on. On the contrary, we may have the SUSY contribution to the muon MDM to be of order $O(10^{-9})$ even if all the superparticles are heavier than, say, 300GeV (see Fig. 4b) in which case we cannot detect the superparticles even by NLC with $\sqrt{s} = 500$GeV. Therefore, we may be able to have a signal of the superparticles by using the muon MDM even if the superparticles are out of the reach of the forthcoming high energy colliders.

Acknowledgement

The author would like to thank J. Hisano and H. Murayama for useful discussions, and C.D. Carone for reading of the manuscript. This work was supported by the Director, Office of Energy Research, Office of High Energy and Nuclear Physics, Division of High Energy Physics of the U.S. Department of Energy under Contract DE-AC03-76SF00098.

A Functions I_N and J_N

In this appendix, we show some useful formulae for the functions I_N and J_N, which are defined as

$$I_N(m_1^2, \cdots, m_N^2) = \int \frac{d^4k}{(2\pi)^4 i} \frac{1}{(k^2 - m_1^2) \cdots (k^2 - m_N^2)}, \tag{40}$$

$$J_N(m_1^2, \cdots, m_N^2) = \int \frac{d^4k}{(2\pi)^4 i} \frac{k^2}{(k^2 - m_1^2) \cdots (k^2 - m_N^2)}. \tag{41}$$

Then, the signs of the functions I_N and J_N are given by

$$(-1)^N I_N(m_1^2, \cdots, m_N^2) > 0, \tag{42}$$

$$(-1)^{N+1} J_N(m_1^2, \cdots, m_N^2) > 0, \tag{43}$$

The functions I_N and I_{N-1} are related as

$$I_N(m_1^2, \cdots, m_N^2) = \frac{1}{m_1^2 - m_N^2} \{ I_{N-1}(m_1^2, \cdots, m_{N-1}^2) - I_{N-1}(m_2^2, \cdots, m_N^2) \}, \tag{44}$$

and the explicit form of I_2 is given by

$$I_2(m_1^2, m_2^2) = -\frac{1}{16\pi^2}\left\{\frac{m_1^2}{m_1^2 - m_2^2}\ln\left(\frac{m_1^2}{\Lambda^2}\right) + \frac{m_2^2}{m_2^2 - m_1^2}\ln\left(\frac{m_2^2}{\Lambda^2}\right)\right\}. \tag{45}$$

Notice that the function I_2 is logarithmically divergent, and hence I_2 defined in eq.(45) depends on a cut-off parameter Λ. However, I_N $(N \geq 3)$ which is iteratively defined by using eq.(44) is independent of Λ, as it should be. In addition, J_N is related to I_N and I_{N-1} as

$$J_N(m_1^2, \cdots, m_N^2) = I_{N-1}(m_1^2, \cdots, m_{N-1}^2) + m_N^2 I_N(m_1^2, \cdots, m_N^2). \tag{46}$$

In the case where all the masses m_1 – m_N are almost degenerate, it is convenient to use the Taylar expansion of I_N. Define

$$\epsilon_i \equiv \frac{\bar{m}^2 - m_i^2}{\bar{m}^2} \quad (i = 1 - N), \tag{47}$$

with $\bar{m}$ being an arbitrary mass scale, then I_N is expanded as

$$\begin{aligned} I_N(m_1^2, \cdots, m_N^2) &= \frac{(-1)^N}{16\pi^2}\frac{1}{\bar{m}^{2(N-2)}}\sum_{p=0}^{\infty}\frac{1}{(N+p-2)(N+p-1)} \\ &\quad \times \sum_{j_1+\cdots+j_N=p} \epsilon_1^{j_1}\cdots\epsilon_N^{j_N} \quad (N \geq 3), \end{aligned} \tag{48}$$

and for $N = 2$,

$$I_2(m_1^2, m_2^2) = -\frac{1}{16\pi^2}\left\{\ln\left(\frac{\bar{m}^2}{\Lambda^2}\right) + 1\right\} + \frac{1}{16\pi^2}\sum_{p=1}^{\infty}\frac{1}{p(p+1)}\sum_{j_1+j_2=p}\epsilon_1^{j_1}\epsilon_2^{j_2}. \tag{49}$$

Notice that eqs.(44) – (49) are useful for numerical calculations.

Furthermore, the function I_N has mass dimension $(4 - 2N)$. Therefore, we obtain

$$\frac{d}{d\lambda}\left\{\lambda^{2-N} I_N(\lambda m_1^2, \cdots, \lambda m_N^2)\right\} = 0, \tag{50}$$

which reduces to

$$(2 - N) I_N(m_1^2, \cdots, m_N^2) + \sum_{i=1}^{N} m_i^2 I_{N+1}(m_1^2, \cdots, m_i^2, m_i^2, \cdots, m_N^2) = 0. \tag{51}$$

Similar formula can be obtained for J_N;

$$(3 - N) J_N(m_1^2, \cdots, m_N^2) + \sum_{i=1}^{N} m_i^2 J_{N+1}(m_1^2, \cdots, m_i^2, m_i^2, \cdots, m_N^2) = 0. \tag{52}$$

References

[1] J. Wess and B. Zumino, *Nucl. Phys.* **B70** (1974) 39.

[2] L. Maiani, *Gif-sur-Yvette Summer School on Particle Physics*, (Natl. Inst. Nucl. Phys. Part. Phys., Paris, 1979);
M.J.G. Veltman, *Acta Phys. Pol.* **B12** (1981) 437.

[3] P. Langacker and M. Luo, *Phys. Rev.* **D44** (1991) 817;
U. Amaldi, W. de Boer and H. Fürstenau, *Phys. Lett.* **B260** (1991) 447.

[4] Particle Data Group, *Phys. Rev.* **D50** (1994) 1173.

[5] A. Czarnecki, B. Krause and W.J. Marciano, *Phys. Rev.* **D52** (1995) 2619.

[6] T. Kinoshita, in *Frontiers of High Energy Spin Physics*, edited by T. Hasegawa *et al.* (Universal Academy Press, Tokyo, 1993) p.9.

[7] M. May, in *Interactions between Particle and Nuclear Physics*, edited by G.M. Bruce (AIP, New York, 1988) p.1168.

[8] P. Fayet, in *Unification of the Fundamental Particles Interactions*, edited by S. Ferrara, J. Ellis and P. van Nierwenhuizen (Plenum, New York, 1980) p. 587;
J.A. Grifols and A. Mendez, *Phys. Rev.* **D26** (1982) 1809;
J. Ellis, J.S. Hagelin and D.V. Nanopoulos, *Phys. Lett.* **B166** (1982) 283;
R. Barbieri and L. Maiani, *Phys. Lett.* **B117** (1982) 203;
D.A. Kosower, L.M. Krauss and N. Sakai, *Phys. Lett.* **B133** (1983) 305;
T.C. Yuan, R. Arnowitt, A.H. Chamseddine and P. Nath, *Z. Phys.* **C26** (1984) 407;
J.C. Romao, A. Barroso, M.C. Bento and G.C. Branco, *Nucl. Phys.* **B250** (1985) 295.

[9] J. Lopez, D.V. Nanopoulos and X. Wang, *Phys. Rev.* **D49** (1991) 366.

[10] U. Chattopadhyay and P. Nath, preprint NSF-ITP-95-64 (hep-ph/9507386).

[11] S. Dimopoulos and H. Georgi, *Nucl. Phys.* **B193** (1981) 150;
N. Sakai, *Z. Phys.* **C11** (1981) 153.

[12] Y. Kawamura, H. Murayama and M. Yamaguchi, *Phys. Lett.* **B324** (1994) 52.

[13] J. Hisano, T. Moroi, K. Tobe, M. Yamaguchi and T. Yanagida, *Phys. Lett.* **B357** (1995) 579;
J. Hisano, T. Moroi, K. Tobe and M. Yamaguchi, preprint LBL-37819 (hep-ph/9510309), to appear in Phys. Rev. **D**.

[14] For review, H.P. Nilles, *Phys. Rep.* **C110** (1984) 1.

[15] J.-P. Derendinger and C.A. Savoy, *Nucl. Phys.* **B237** (1984) 307.

[16] L3 Collaboration, *Phys. Lett.* **B350** (1995) 109.

Figure caption

Figure 1: Feynman diagrams which give rise to the muon MDM in the mass eigenstate basis. The external lines represent the muon (straight) and the photon (wavy).

Figure 2: Feynman diagrams which give rise to the muon MDM in the mass insertion method.

Figure 3: The SUSY contribution to the muon MDM, $\Delta a_\mu^{\rm SUSY}$, in μ_H-m_{G2} plane. The right-handed smuon mass is taken to be $m_{\tilde{\mu}R} = 100$GeV. We take $\tan\beta = 30$, and the left handed smuon mass $m_{\tilde{\mu}L}$ is (a) 100GeV, (b) 300GeV and (c) 500GeV. The numbers given in the figures represent the value of $\Delta a_\mu^{\rm SUSY}$ in units of 10^{-9}.

Figure 4: Same as Fig. 3 except for $m_{\tilde{\mu}R} = 300$GeV.

Figure 5: Same as Fig. 3 except for $m_{\tilde{\mu}R} = 1$TeV.

Figure 6: The SUSY contribution to the muon MDM, $\Delta a_\mu^{\rm SUSY}$, in μ_H-m_{G2} plane. The right-handed smuon mass $m_{\tilde{\mu}R}$ is determined so that $\Delta a_\mu^{\rm SUSY}$ takes its minimal value. We take $\tan\beta = 30$, and the left handed smuon mass $m_{\tilde{\mu}L}$ is taken to be (a) 100GeV, (b) 200GeV, (c) 300GeV and (d) 500GeV. The numbers given in the figures represent the value of $\Delta a_\mu^{\rm SUSY}$ in units of 10^{-9}.

Figure 7: Contours which gives the threshold value, *i.e.* $\Delta a_\mu^{\rm SUSY} = -9.0 \times 10^{-9}$ (dotted line) and $\Delta a_\mu^{\rm SUSY} = 19.0 \times 10^{-9}$ (solid line). The right-handed smuon mass $m_{\tilde{\mu}R}$ is determined so that $|\Delta a_\mu^{\rm SUSY} - 5.0 \times 10^{-9}|$ is minimized. The values shown in the figures represent those of $\tan\beta$, and we take the left handed smuon mass $m_{\tilde{\mu}L}$ to be (a) 100GeV, (b) 200GeV and (c) 300GeV.

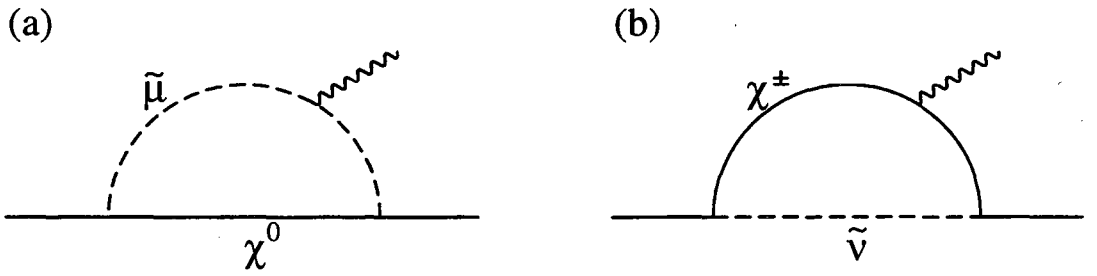
(a)
$\tilde{\mu}$
χ^0
(b)
$\chi^{\pm}$
$\tilde{\nu}$

Fig. 1

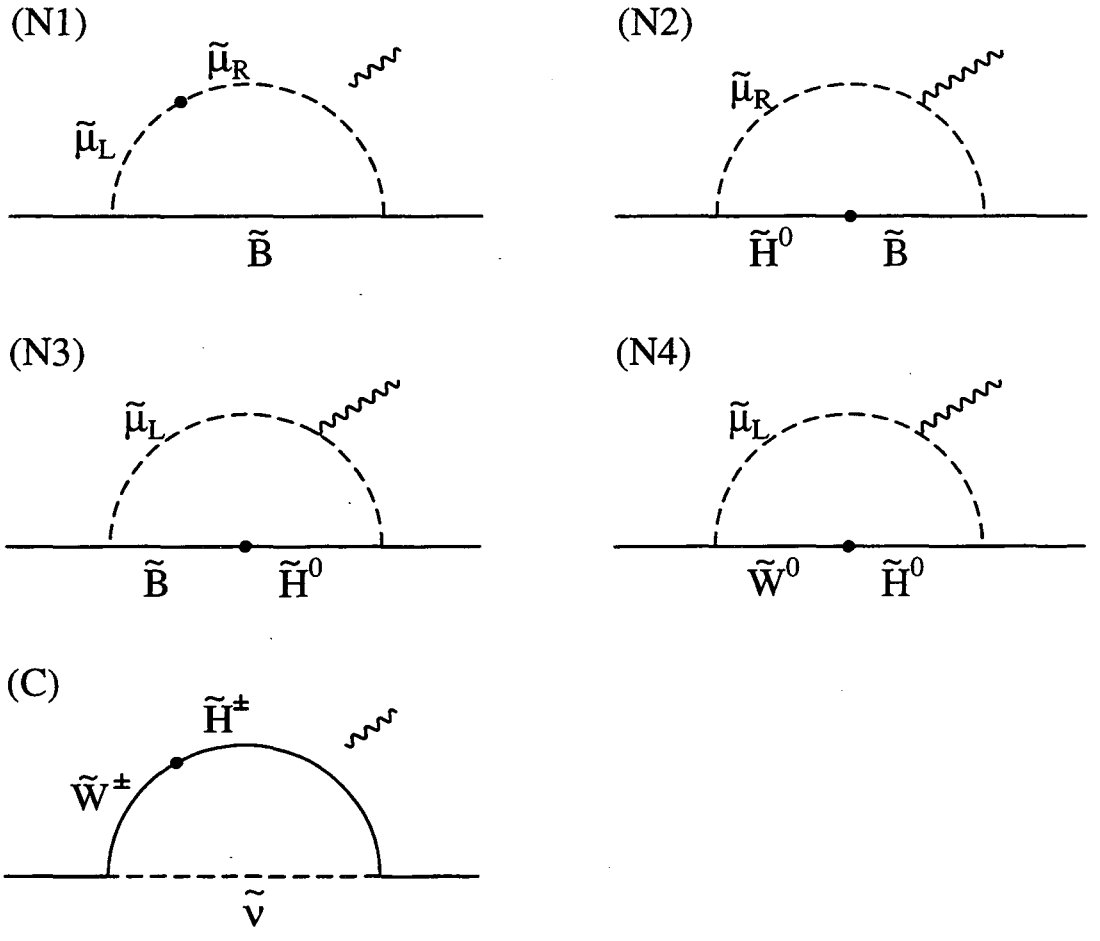
(N1)
$\tilde{\mu}_R$
$\tilde{\mu}_L$
$\tilde{B}$
(N2)
$\tilde{\mu}_R$
$\tilde{H}^0$
$\tilde{B}$
(N3)
$\tilde{\mu}_L$
$\tilde{B}$
$\tilde{H}^0$
(N4)
$\tilde{\mu}_L$
$\tilde{W}^0$
$\tilde{H}^0$
(C)
$\tilde{H}^{\pm}$
$\tilde{W}^{\pm}$
$\tilde{\nu}$

Fig. 2

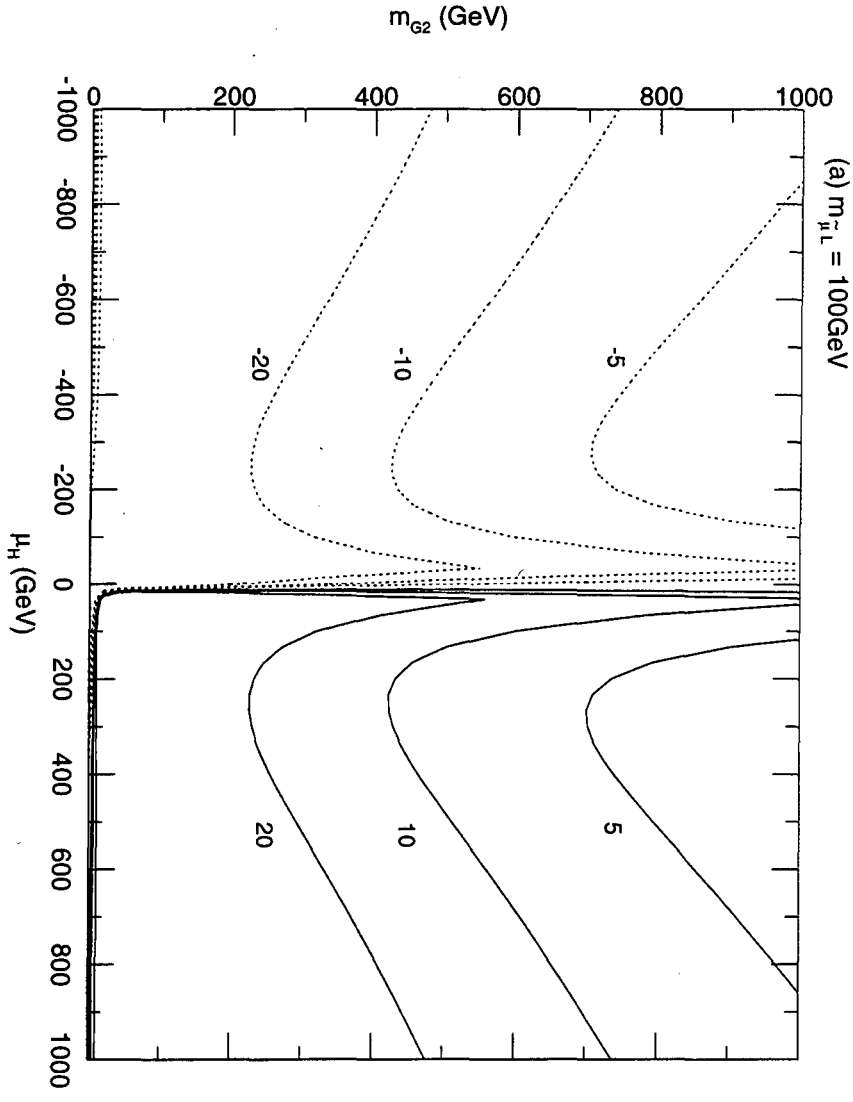
(a) $m_{\tilde{\mu}_L}$ = 100GeV
-5
-10
-20
5
10
20
m_{G2} (GeV)
0
200
400
600
800
1000
μ_H (GeV)
-1000
-800
-600
-400
-200
0
200
400
600
800
1000

Fig. 3a

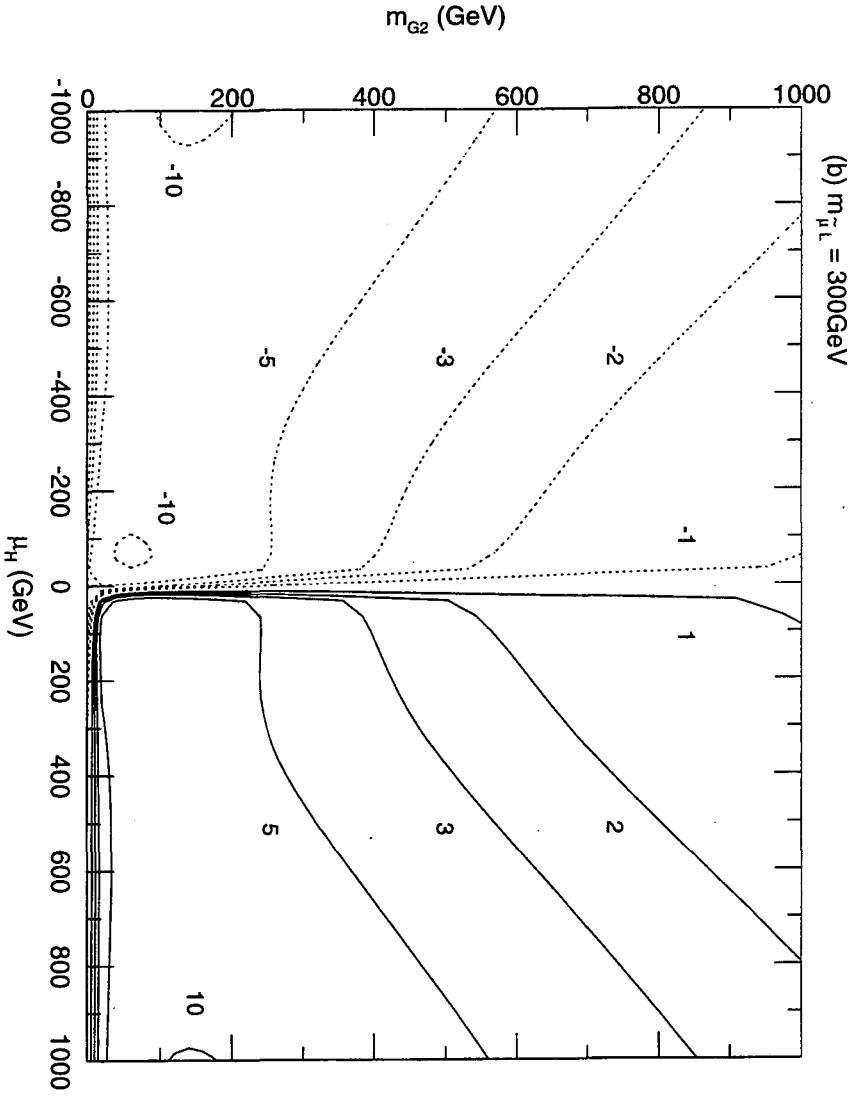
(b) $m_{\tilde{\mu}_L}$ = 300GeV
m_{G2} (GeV)
μ_H (GeV)
0
200
400
600
800
1000
-1000
-800
-600
-400
-200
0
200
400
600
800
1000
-1
-2
-3
-5
-10
1
2
3
5
10

Fig. 3b

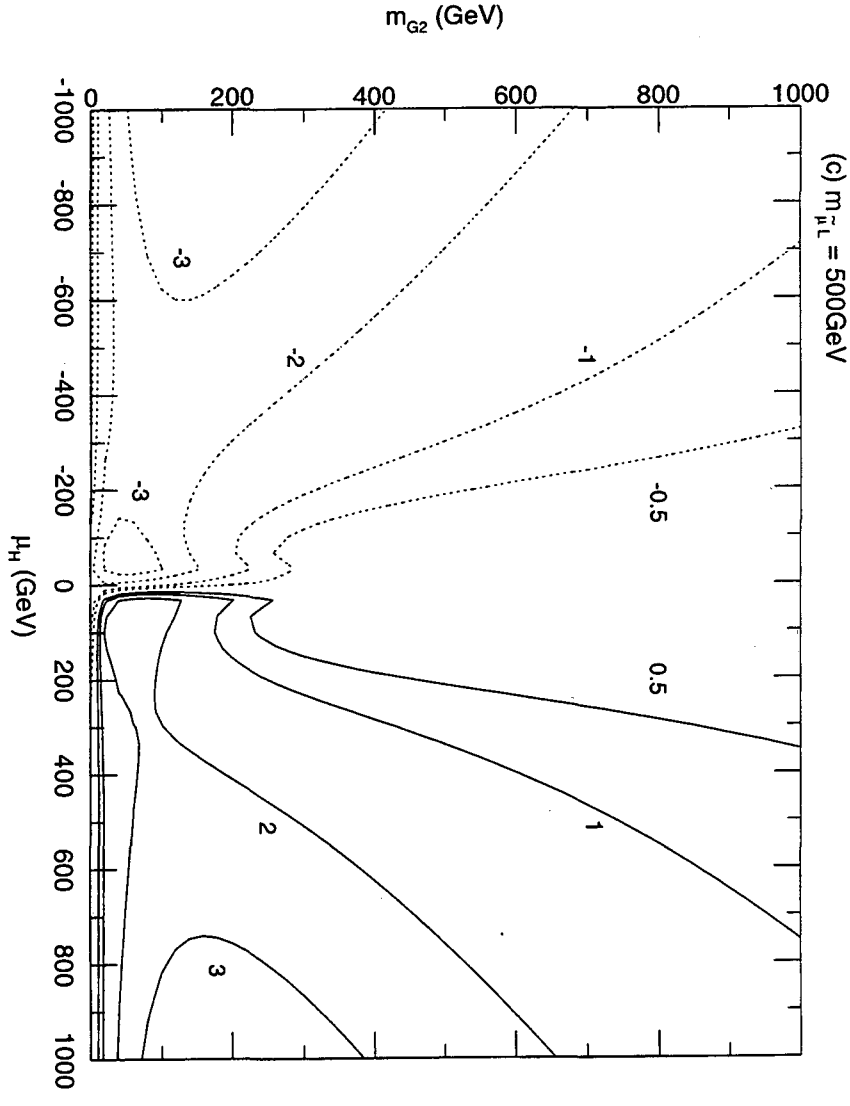
(c) $m_{\tilde{\mu}_L}$ = 500GeV
m_{G2} (GeV)
μ_H (GeV)
0
200
400
600
800
1000
-1000
-800
-600
-400
-200
0
200
400
600
800
1000
-3
-2
-1
-0.5
-3
0.5
1
2
3

Fig. 3c

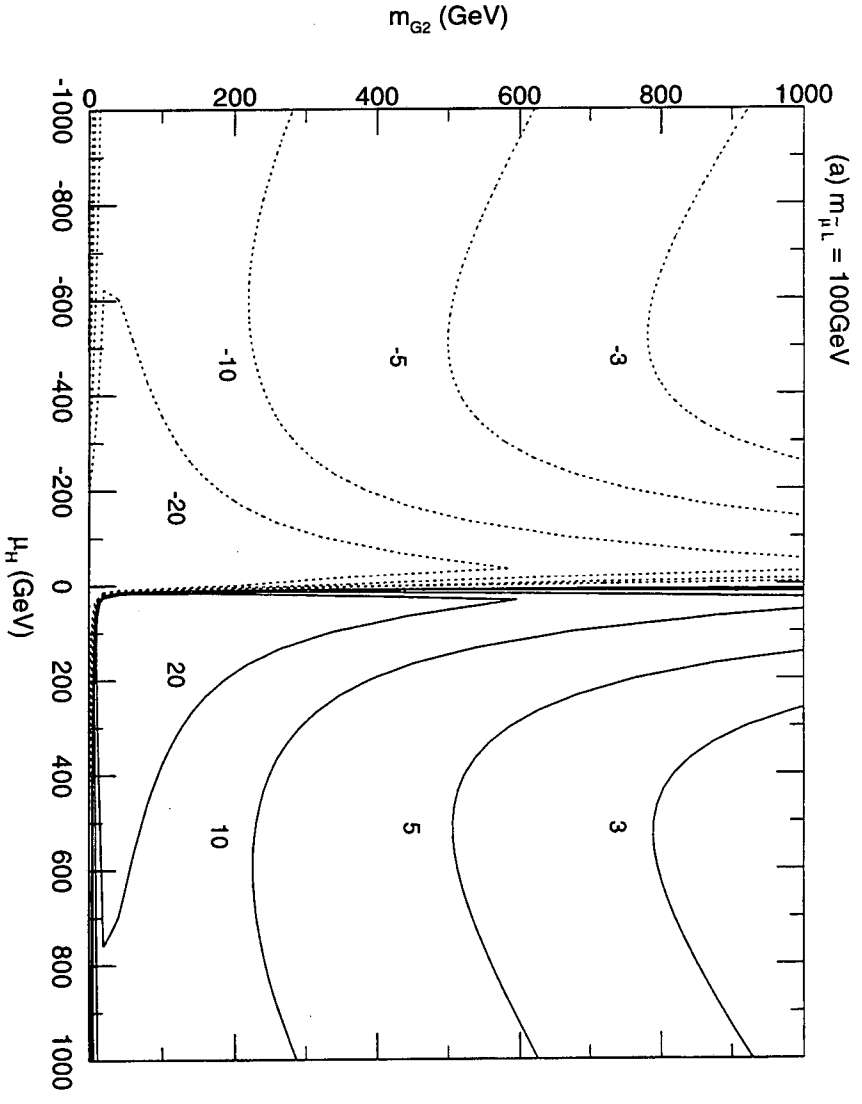
(a) $m_{\tilde{\mu}_L}$ = 100GeV
-3
-5
-10
-20
3
5
10
20
m_{G2} (GeV)
0
200
400
600
800
1000
μ_H (GeV)
-1000
-800
-600
-400
-200
0
200
400
600
800
1000

Fig. 4a

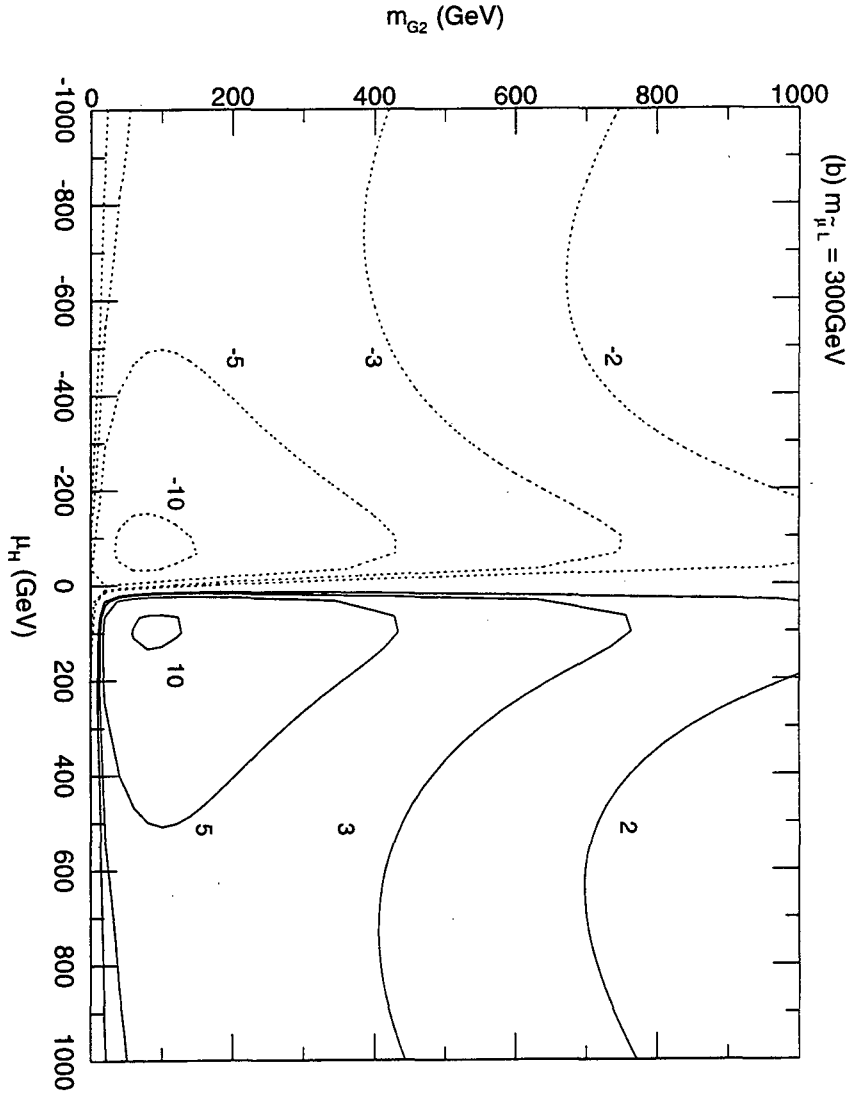
(b) $m_{\tilde{\mu}_L}$ = 300GeV
m_{G2} (GeV)
μ_H (GeV)
0
200
400
600
800
1000
-1000
-800
-600
-400
-200
0
200
400
600
800
1000
-2
-3
-5
-10
2
3
5
10

Fig. 4b

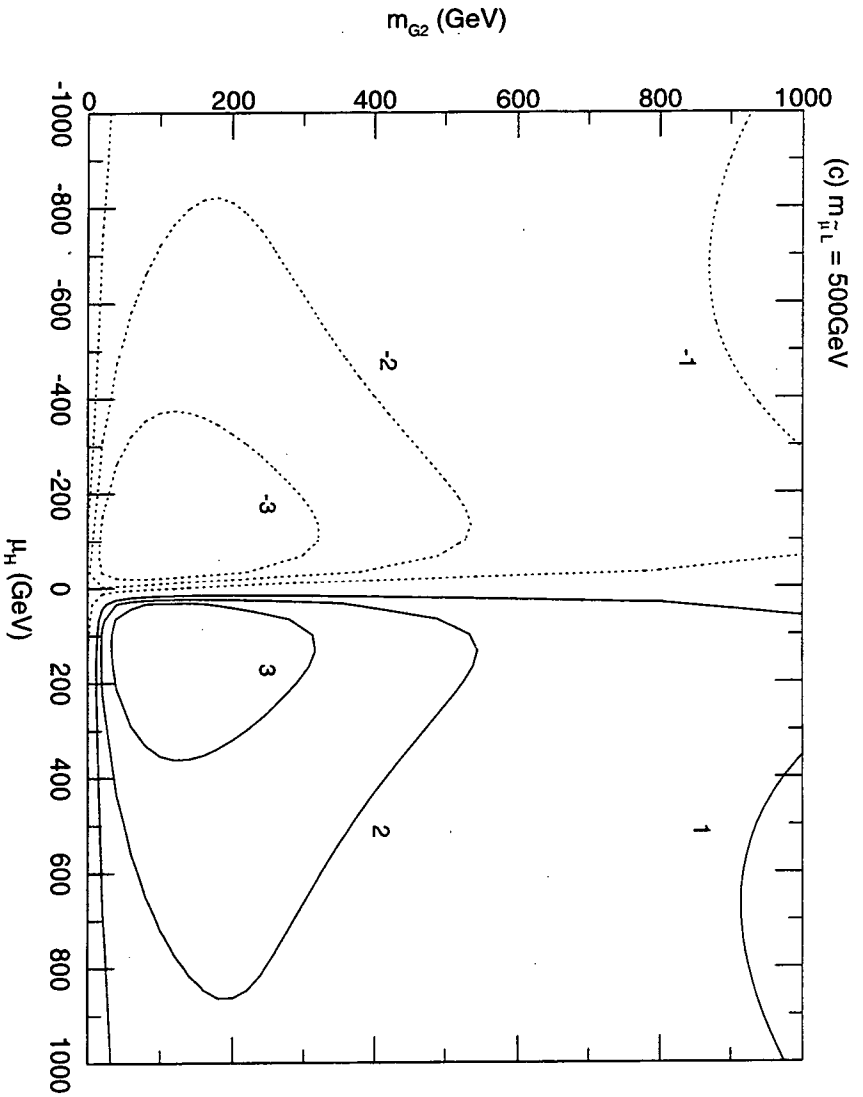
(c) $m_{\tilde{\mu}_L}$ = 500GeV
m_{G2} (GeV)
μ_H (GeV)
0
200
400
600
800
1000
-1000
-800
-600
-400
-200
0
200
400
600
800
1000
-1
-2
-3
1
2
3

Fig. 4c

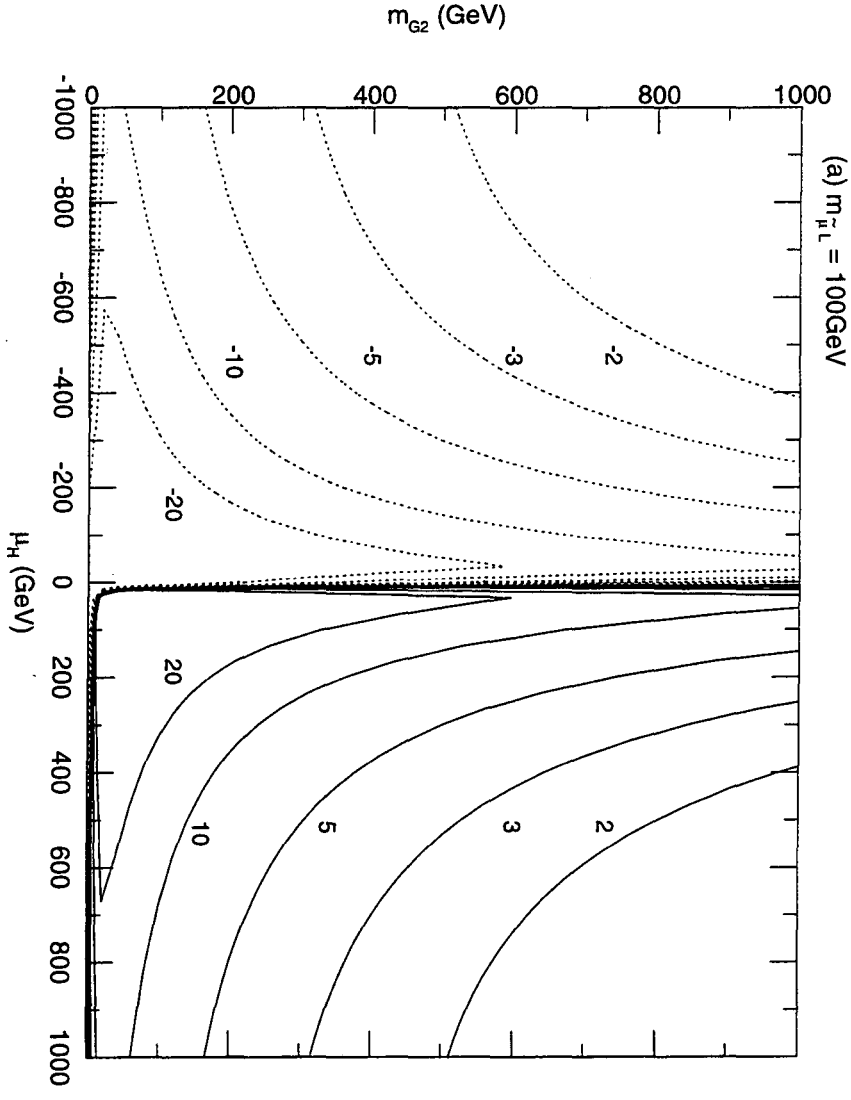
(a) $m_{\tilde{\mu}_L}$ = 100GeV
m_{G2} (GeV)
μ_H (GeV)
0
200
400
600
800
1000
-1000
-800
-600
-400
-200
0
200
400
600
800
1000
-2
-3
-5
-10
-20
2
3
5
10
20

Fig. 5a

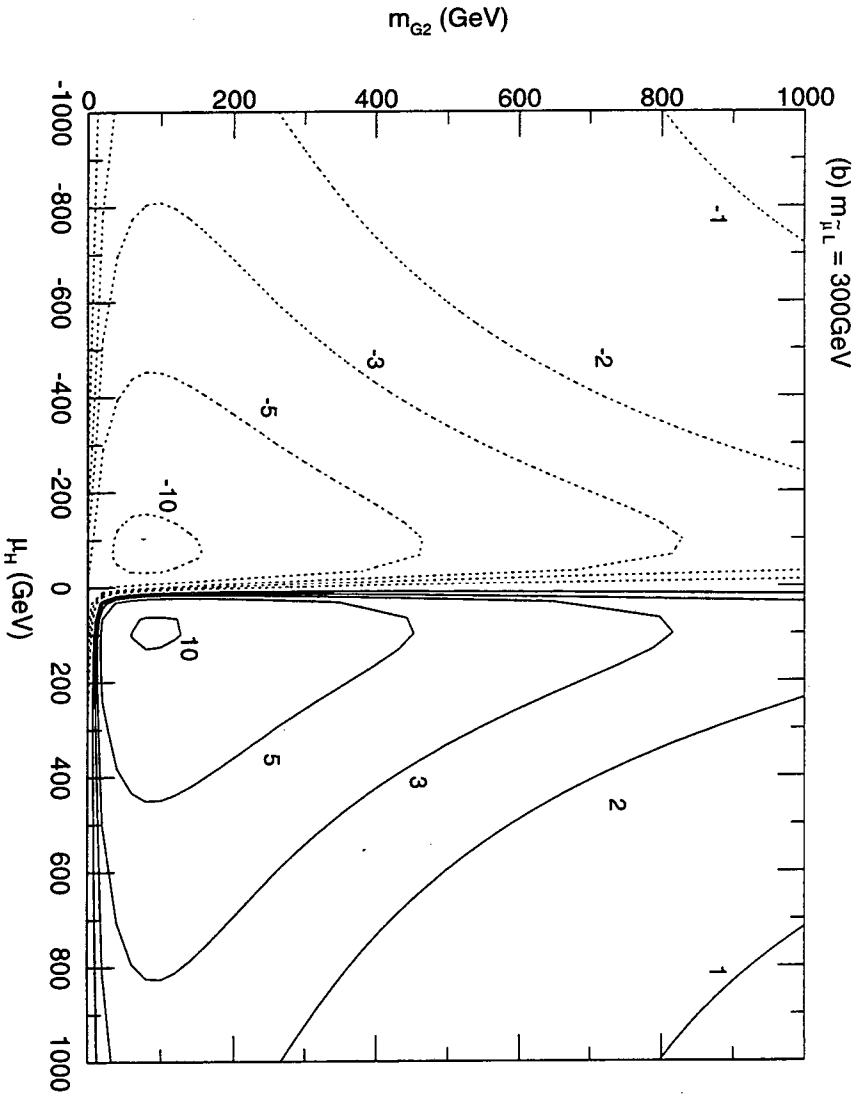
(b) $m_{\tilde{\mu}_L}$ = 300GeV
m_{G2} (GeV)
μ_H (GeV)
0
200
400
600
800
1000
-1000
-800
-600
-400
-200
0
200
400
600
800
1000
-1
-2
-3
-5
-10
10
5
3
2
1

Fig. 5b

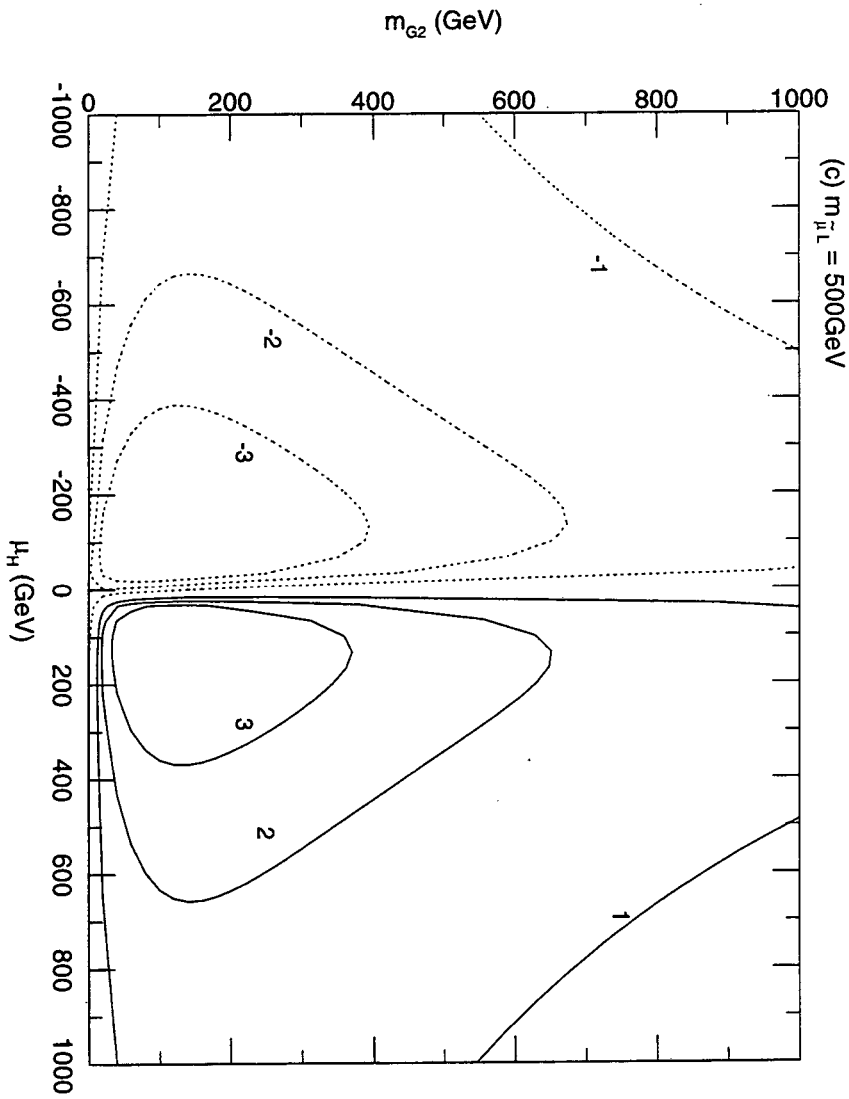
(c) $m_{\tilde{\mu}_L}$ = 500GeV
μ_H (GeV)
-1000
-800
-600
-400
-200
0
200
400
600
800
1000
m_{G2} (GeV)
0
200
400
600
800
1000
-1
-2
-3
3
2
1

Fig. 5c

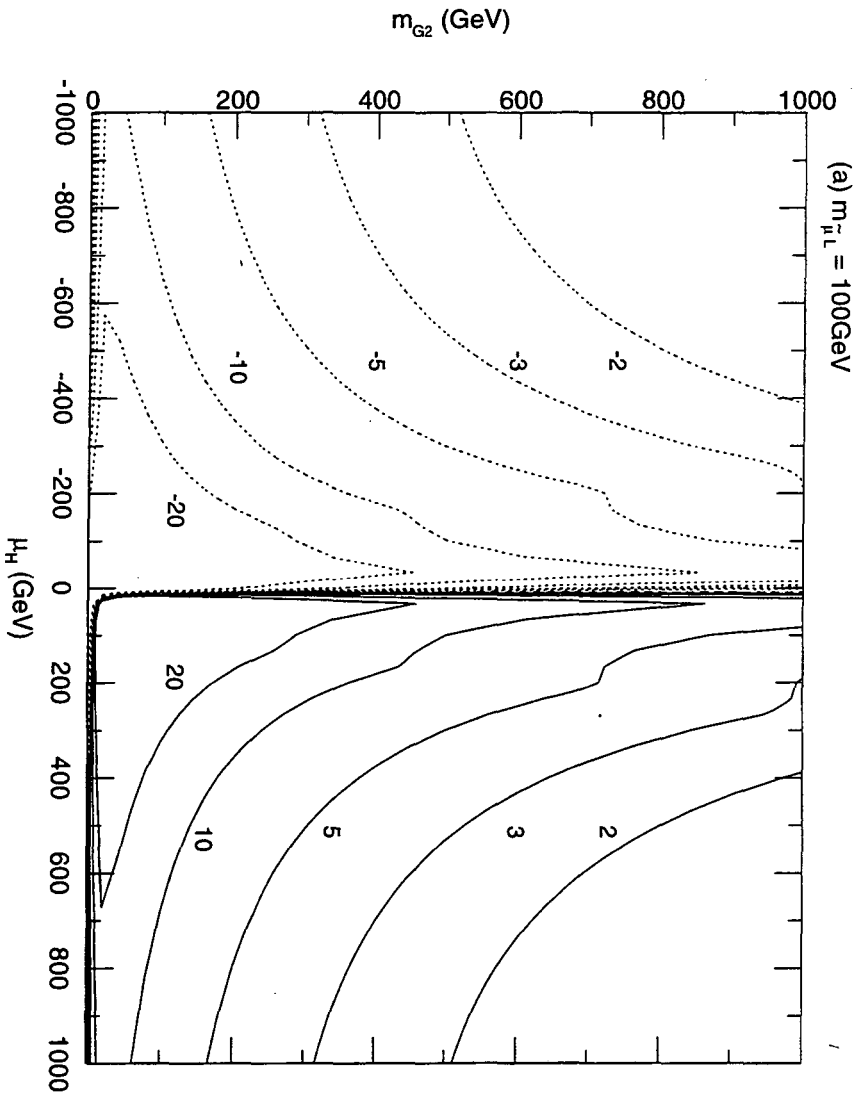
(a) $m_{\tilde{\mu}_L}$ = 100GeV
m_{G2} (GeV)
0
200
400
600
800
1000
μ_H (GeV)
-1000
-800
-600
-400
-200
0
200
400
600
800
1000
-2
-3
-5
-10
-20
2
3
5
10
20

Fig. 6a

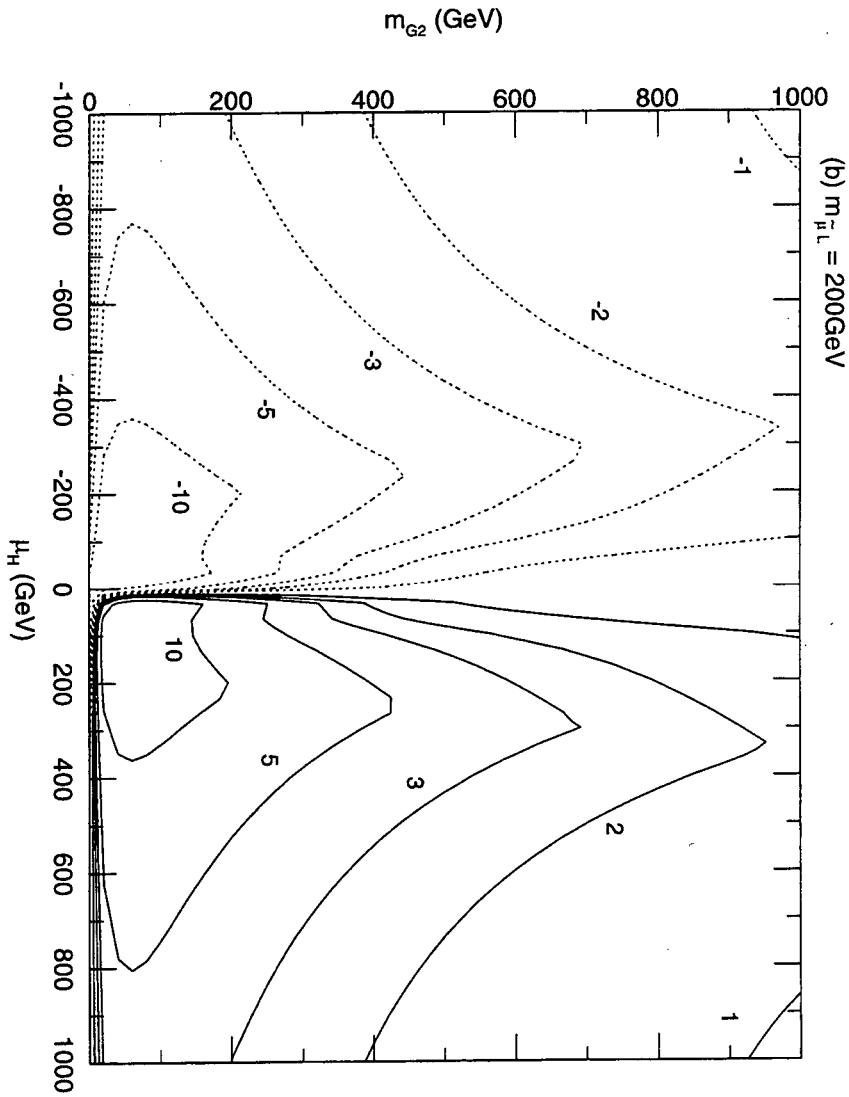
(b) $m_{\tilde{\mu}_L}$ = 200GeV
m_{G2} (GeV)
μ_H (GeV)
0
200
400
600
800
1000
-1000
-800
-600
-400
-200
0
200
400
600
800
1000
-1
-2
-3
-5
-10
1
2
3
5
10

Fig. 6b

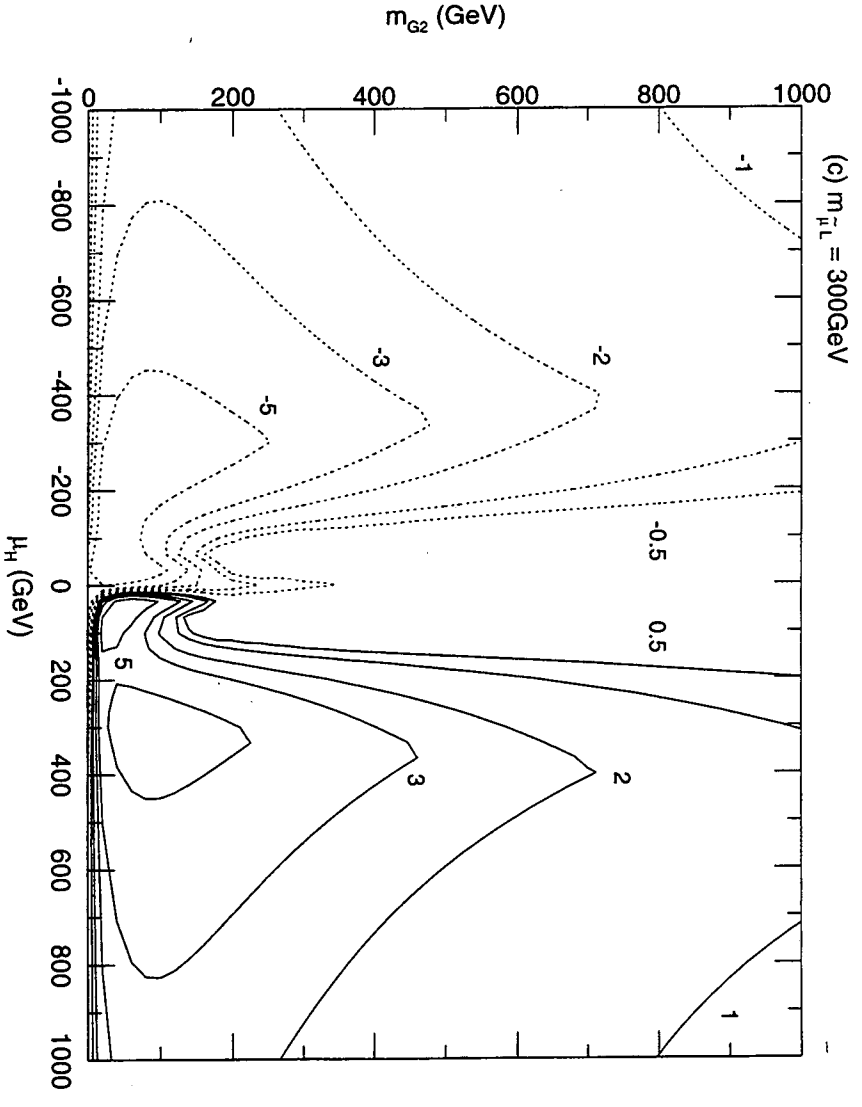
(c) $m_{\tilde{\mu}_L}$ = 300GeV
m_{G2} (GeV)
μ_H (GeV)
0
200
400
600
800
1000
-1000
-800
-600
-400
-200
0
200
400
600
800
1000
-1
-2
-3
-5
-0.5
0.5
1
2
3
5

Fig. 6c

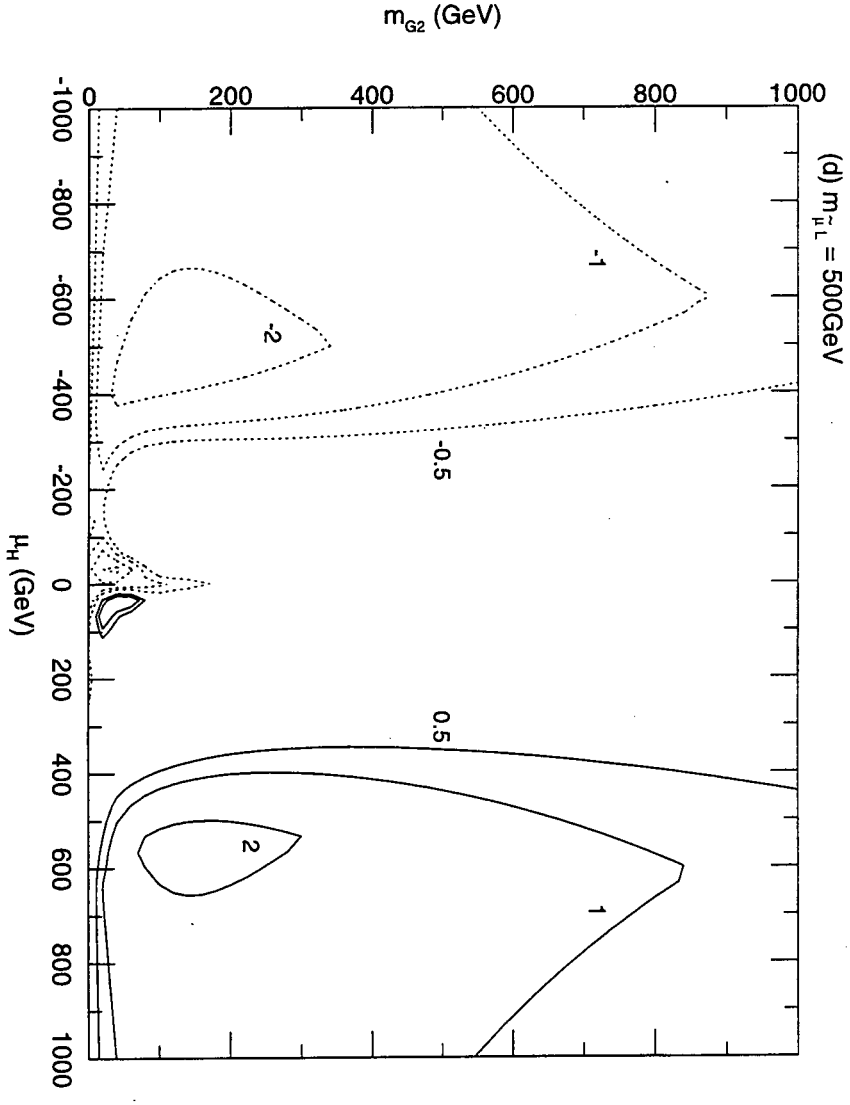
(d) $m_{\tilde{\mu}_L}$ = 500GeV
m_{G2} (GeV)
μ_H (GeV)
0
200
400
600
800
1000
-1000
-800
-600
-400
-200
0
200
400
600
800
1000
-1
-2
-0.5
0.5
2
1

Fig. 6d

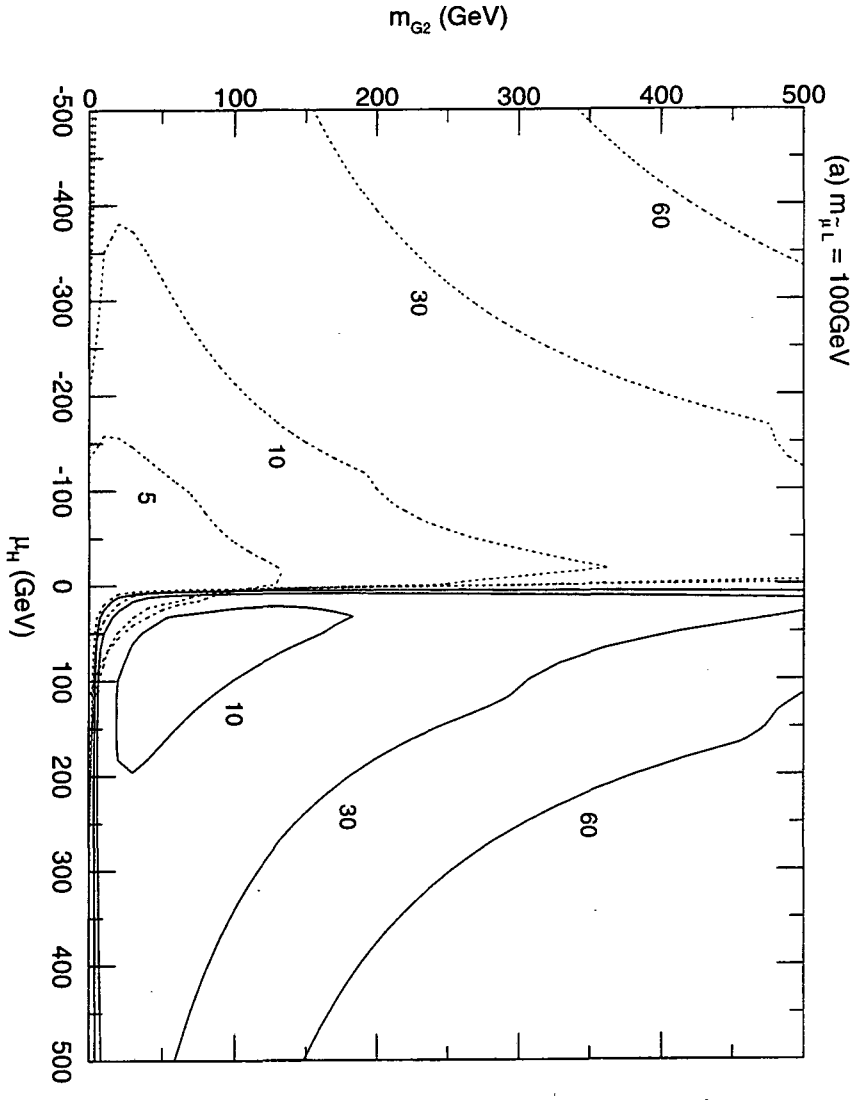
(a) $m_{\tilde{\mu}_L}$ = 100GeV
60
30
10
5
10
30
60
μ_H (GeV)
-500
-400
-300
-200
-100
0
100
200
300
400
500
m_{G2} (GeV)
0
100
200
300
400
500

Fig. 7a

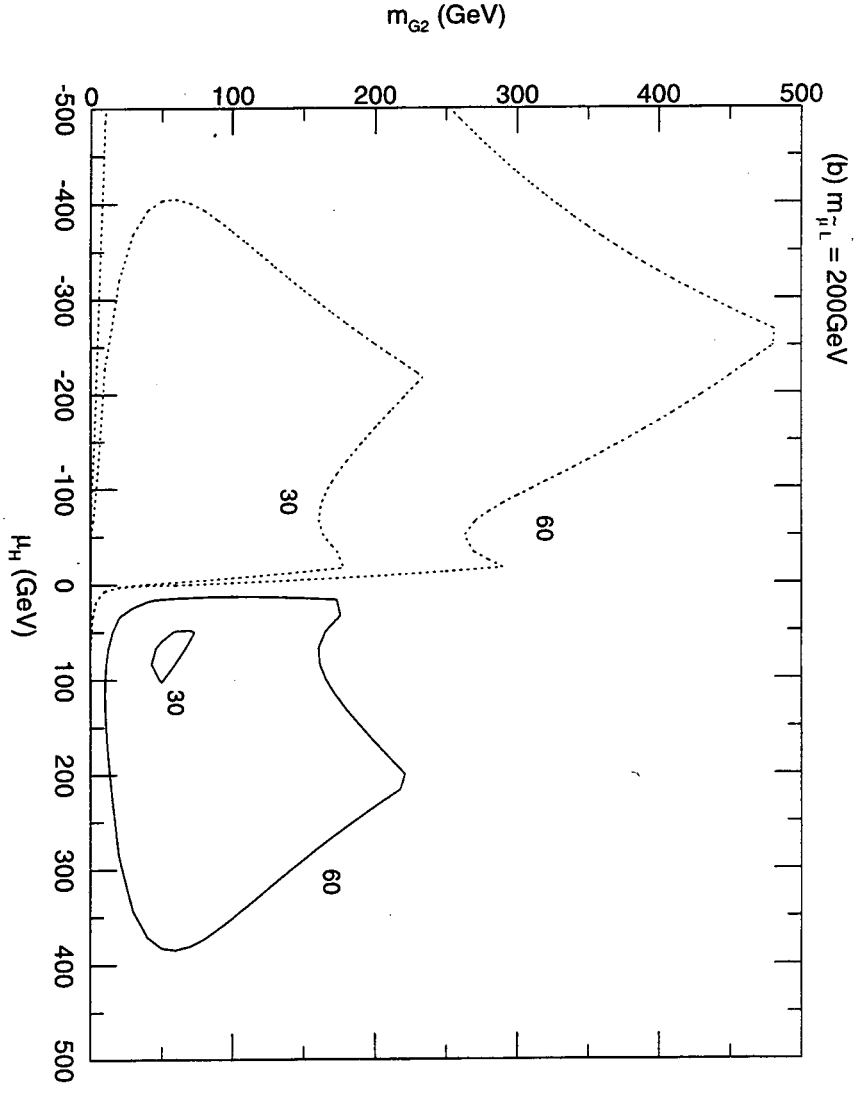
(b) $m_{\tilde{\mu}_L}$ = 200GeV
m_{G2} (GeV)
μ_H (GeV)
0
100
200
300
400
500
-500
-400
-300
-200
-100
0
100
200
300
400
500
30
60
30
60

Fig. 7b

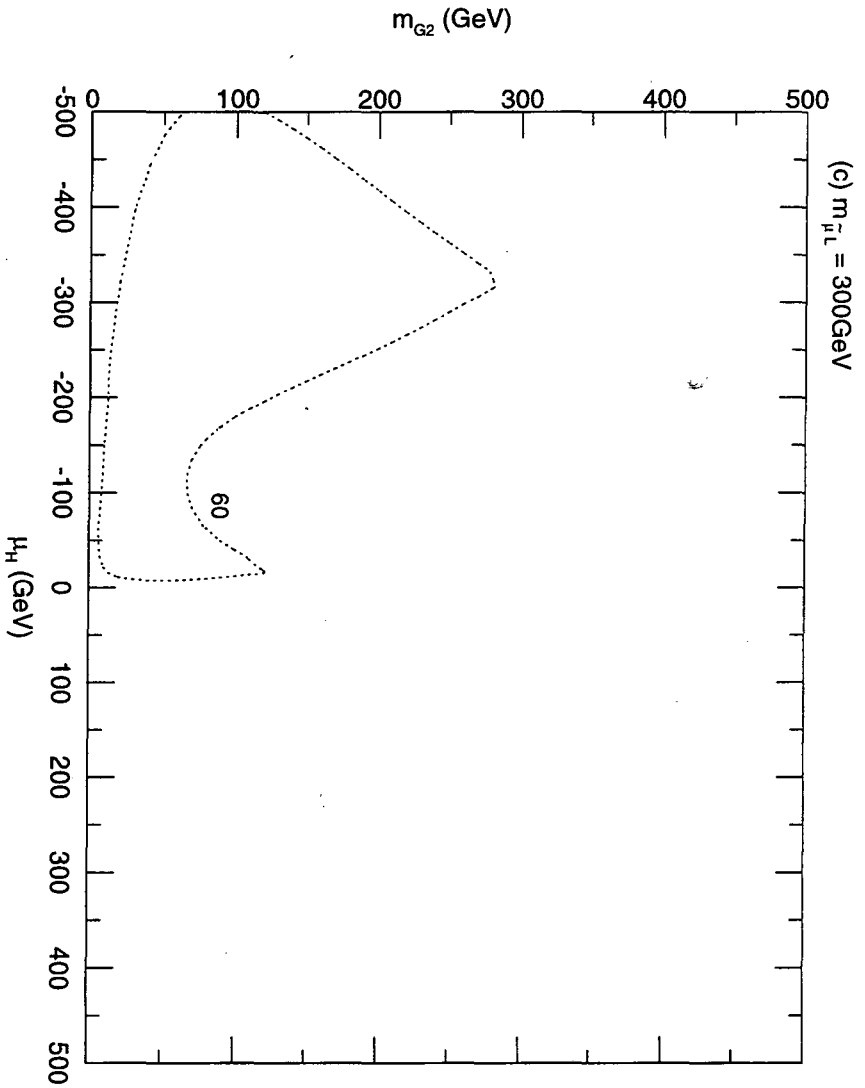
(c) $m_{\tilde{\mu}_L}$ = 300GeV
μ_H (GeV)
-500
-400
-300
-200
-100
0
100
200
300
400
500
m_{G2} (GeV)
0
100
200
300
400
500
60

Fig. 7c

Ernest Orlando Lawrence Berkeley National Laboratory
Technical and Electronic Information Department
University of California | Berkeley, California 94720